The Pharmacological Effect of Two Antibody Drugs for the Treatment of Tumor Metastasis

A Dissertation Submitted to
the Graduate School of Life and Environmental Sciences,
the University of Tsukuba
in Partial Fulfillment of the Requirements
for the Degree of Doctor of Philosophy in Biological Science
(Doctoral Program in Biological Sciences)

Kenji KASHIMA

Abbreviations

CHO:	Chinese hamster ovary
DMSO:	dimethyl sulfoxide
GAPDH:	glyceraldehyde-3-phosphate dehydrogenase
HEK:	human embryonic kidney
PBS:	phosphate-buffered saline
PCR:	polymerase chain reaction
VEGF:	vascular endothelial growth factor
CXCR:	CXC chemokine receptor
SDF1:	stromal cell-derived factor 1
VEGFR:	vascular endothelial growth factor receptor
CD44:	cluster of designation or classification determinant 44
LYVE-1:	lymphatic vessel endothelial hyaluronan receptor-1
HAT:	hypoxanthine-aminopterin-thymidine
HRP:	horseradish peroxidase
FBS:	fetal bovine serum
HBSS:	Hank's Balanced Salt Solution
MAb:	monoclonal antibody
ELISA:	enzyme-linked immuno-sorbent assay
O.C.T:	optimal cutting temperature
IHC:	immunohistochemistry
CXCL:	C-X-C motif ligand
cAMP:	cyclic adenosine 3′,5′-monophosphate
IBMX:	3-Isobutyl-1-methylanxthine
MMPs:	matrix metalloproteinase
HGF:	hepatocyte growth factor
EMT:	epithelial-mesenchymal transition
HER2:	human epidermal growth factor receptor 2
cDNA:	complementary deoxyribonucleic acid
IgG:	Immunoglobulin G
Ig:	Immunoglobulin
SCID mice:	C.B-17/Icr-scid Jcl
FFPE:	formalin-fixed paraffin-embedded
DAB:	3,3′-diaminobenzidine

mRNA:	messenger ribonucleic asid
siRNA:	small interfering ribonucleic asid
CD31:	cluster of designation or classification determinant 31
HMVEC-Lly:	Human lung lymphatic microvascular endothelial cells
FACS:	fluorescence activated cell sorting
FRET:	Fluorescence resonance energy transfer
Nude mice:	CAnN.Cg-Foxn1<nu>/CrlCrlj nu/nu

INDEX

Contents **Pages**

Abstract

Cancer is the most common cause of death in Japan since 1981. Cancer death is deeply associated with tumor metastasis. The lethality of patients with metastatic diseases is much higher than that of patients with localized tumors. Therefore, therapeutic modalities capable of inhibiting tumor metastasis would be beneficial for the treatment of many tumors. However, to date, no anti-metastatic drug is available. The objectives of this study were to generate novel drug candidates that have antitumor metastatic activity.

In Chapter I, the author developed an anti-VEGF-D monoclonal antibody, cVE199, and investigated its *in vitro* properties, *in vivo* effects against tumors, and possible target indications. VEGF-D has been implicated in the promotion of the metastatic potential of several tumors. The cVE199 molecule specifically bound to human VEGF-D. In addition, cVE199 inhibited the biological activity of VEGF-D/VEGFR-3 signal transduction *in vitro*. Because the author determined that a neuroblastoma cell line, SK-N-DZ, abundantly expressed VEGF-D, an *in vivo* efficacy study was performed using a SK-N-DZ xenograft model. cVE199 significantly decreased SK-N-DZ lymphatic metastasis. Finally, the author investigated VEGF-D expression in human neuroblastoma and determined that the molecule was expressed in 11 out of 29 human neuroblastoma specimens (37.9%). In conclusion, in Chapter I, the author found that a novel anti-VEGF-D monoclonal antibody, cVE199, with specific reactivity against human VEGF-D, prevents lymphatic metastasis of neuroblastoma in an animal model. In addition, my results show that VEGF-D is expressed in some cases of human neuroblastoma, which suggests that cVE199 is a potential anti-metastatic therapeutic antibody for neuroblastoma treatment.

In Chapter II, the author developed a novel anti-CXCR4 monoclonal antibody, CF172,

and investigated its anti-metastatic activity against rhabdomyosarcoma cells. CXCR4 has been implicated in the promotion of the metastatic potential of rhabdomyosarcoma. The CF172 molecule specifically bound to human CXCR4 and neutralized CXCR4/SDF1 signal transduction. Using CF172, the author determined that the rhabdomyosarcoma cell line, SJCRH30, expressed high levels of CXCR4. In addition, CF172 inhibited the SDF1-induced migration activity of SJCRH30 cells *in vitro*. Using SJCRH30 xenograft models, the author performed *in vivo* efficacy studies for peritoneal and lymph node metastasis, which are clinically observed in rhabdomyosarcoma. These studies indicated that CF172 significantly decreased both types of metastasis. In conclusion, in Chapter II, the author found that a novel anti-CXCR4 monoclonal antibody, CF172, with specific reactivity against human CXCR4, prevented peritoneal metastasis and lymph node metastasis of rhabdomyosarcoma in animal models. These results suggest that CF172 is a potential anti-metastatic therapeutic antibody for rhabdomyosarcoma treatment.

In conclusion, the author identified two monoclonal antibodies, cVE199 and CF172, which specifically target VEGF-D and CXCR4, respectively. Both antibodies presented antitumor metastasis activities in animal models. These data suggest that these antibodies are promising anti-metastatic therapeutics for cancer treatment.

General Introduction

Cancer is a disease, which involves abnormal cell growth with the potential to invade or spread to other parts of the body (Dudjak 1992). Cancer is the most common cause of death in Japan since 1981. Molecular targeted therapy (e.g., anti-HER2 antibody: trastuzumab) improved treatment results for some tumor types. However, these improvements are still limited (Allemani et al. 2015). Therefore, it is still important to generate novel antitumor drugs.

Metastasis is of great importance for the clinical management of cancer since cancer mortality is mainly associated with disseminated disease rather than with the primary tumor (Fidler 1999). Therefore, therapeutic modalities capable of inhibiting tumor metastasis would be beneficial for the treatment of many tumors. However, to date, no anti-metastatic drug is available. In fact, metastasis is an extraordinarily complex process. To successfully colonize a secondary site, a cancer cell must complete a sequential series of steps before it becomes a clinically detectable lesion. The details of the mechanisms of tumor metastasis are as follows: (a) proliferation of tumors within the primary site, (b) detachment from the primary site and invasion into the blood/lymphatic vessels, (c) chemotaxis in the vessels, and (d) provide a favorable microenvironment for tumor cell survival and growth (Fidler and Ellis 2000, Fidler 2002, Yeung et al. 2015).

Based on these information, the author focused on the lymphatic vessels (categorized in step (b)) and chemotaxis (categorized in step (c)) to generate novel anti-metastatic drugs. Lymphatic metastasis, defined by the invasion of the lymph nodes by cancer cells, is known as the first step of metastasis in most cancers. Lymphatic vessels are important factors for lymphatic metastasis because most vessels that directly connect to lymph nodes are lymphatic vessels (Stacker et al. 2014). Indeed, there is a positive correlation

between tumor lymphatic vessel density and lymphatic metastasis (Frech et al. 2009, Chung et al. 2010). Therefore, the author attempted to generate an anti-lymphangiogenic antibody as an anti-metastatic drug. A novel member of the vascular endothelial growth factor (VEGF) family, namely VEGF-D, has been implicated in the promotion of lymphangiogenesis. In general, VEGF-D binds to the VEGF receptor (VEGFR)-2, found on both the blood and lymphatic vessels, and VEGFR-3, found predominantly on the lymphatic vessels and in some angiogenic tumor blood vessels (Achen et al. 1998, Saharinen et al. 2004). VEGFR-3 signaling is the primary factor responsible for the lymphangiogenic response to VEGF-D stimulation and leads to lymphangiogenesis in mouse models (Veikkola et al. 2001). Several experimental and clinical studies indicated positive correlations between VEGF-D expression, tumor lymphatic vessel density, and lymphatic metastasis (Achen and Stacker 2008). Moreover, a number of reports showed that higher VEGF-D expression correlates with poor prognosis in human tumors (White et al. 2002, Nakamura et al. 2003, Yokoyama et al. 2003, Juttner et al. 2006, Liu et al. 2008). Therefore, VEGF-D blockade seems to be a promising method to prevent lymphatic metastasis of tumors.

Regarding chemotaxis during tumor metastasis, chemokines, small pro-inflammatory chemoattractant proteins that bind to G-protein coupled receptors present on the cell surfaces of target cells, are major regulators of cell trafficking (Bockhorn et al. 2007). The chemokine, stromal cell-derived factor 1 (SDF1), and its receptor, CXC chemokine receptor-4 (CXCR4), play a unique role in homing and migration of hematopoietic and lymphopoietic cells (Kucia et al. 2004, Strahm et al. 2008). In addition, studies suggested that CXCR4 may be involved in the promotion of the metastatic potential of multiple tumor types, by activating migration and homing of tumors (Muller et al. 2001, Burger

and Kipps 2006, Oda et al. 2007, Akashi et al. 2008, Joyce and Pollard 2009). Moreover, results of a recently published study indicated that high levels of CXCR4 expression in rhabdomyosarcoma correlated with metastatic potential and poor prognosis (Diomedi-Camassei et al. 2008). Therefore, blocking CXCR4 would be a promising approach in the treatment of metastatic rhabdomyosarcoma.

To explore these possibilities, the author generated novel neutralizing antibodies, cVE199 and CF172, which are targeting VEGF-D and CXCR4, respectively. Additionally, the author investigated the *in vitro* activities and anti-metastatic efficacies of these two antibodies in animal models and their possible indications for human cancer treatment.

Chapter I: Blockade of VEGF-D by cVE199 Inhibits Lymphatic Metastasis in Neuroblastoma

1. Introduction

Cancer lethality is primarily associated with metastasis (Liotta 1992). In one type of metastasis, known as lymphatic metastasis, cancer cells spread to the lymph nodes. This type of metastasis serves as an important prognostic indicator for the disease state and lymphatic metastasis is correlated with poor prognosis in many cancer types (Grandi et al. 1985, de Manzoni et al. 1996, Qin and Tang 2002, Ghaferi et al. 2009, Lughezzani et al. 2009, Tuna et al. 2011).

Multiple steps are required for lymphatic metastasis to occur, including detachment from the primary tumor mass; invasion into lymphatic vessels; transport through draining lymphatic vessels; and finally arrest, survival, and growth in the lymph nodes (Nguyen 2004, Pantel and Brakenhoff 2004). The first step is the formation of a new lymphatic vasculature from preexisting vessels in tumors, a process called lymphangiogenesis. Reliable markers for lymph vessels such as CD44-related hyaluronan receptor LYVE-1 revealed that tumor-associated upregulation of lymphangiogenesis is linked to increased lymphatic spread and poor prognosis in human cancers (Raica and Ribatti 2010). Hence, lymphangiogenesis has become the focus of interest in lymphatic metastasis research.

A novel member of the vascular endothelial growth factor (VEGF) family, namely VEGF-D, has been implicated in the promotion of lymphangiogenesis. This molecule is synthesized as a proprotein. Following synthesis, the VEGF homology domain region is proteolytically cleaved and secreted into the extracellular environment. This

processing progressively increases the affinity of the molecule for its receptors (Stacker et al. 1999). In general, VEGF-D binds to the VEGF receptor (VEGFR)-2, expressed on both blood and lymphatic vessels, and VEGFR-3, predominantly expressed on lymphatic vessels and in some angiogenic tumor blood vessels (Achen et al. 1998, Saharinen et al. 2004). VEGFR-3 signaling is the primary factor responsible for the lymphangiogenic response to VEGF-D stimulation and leads to lymphangiogenesis in mouse models (Veikkola et al. 2001). Several experimental and clinical studies indicated positive correlations between VEGF-D expression, tumor lymphatic vessel density, and lymphatic metastasis (Achen and Stacker 2008). Moreover, a number of reports showed that higher VEGF-D expression correlates with poor prognosis in human tumors (White et al. 2002, Nakamura et al. 2003, Yokoyama et al. 2003, Juttner et al. 2006, Liu et al. 2008). Therefore, VEGF-D blockade seems to be a promising method to prevent lymphatic metastasis.

To explore this possibility, the author generated a novel anti-VEGF-D monoclonal antibody, cVE199, and investigated its *in vitro* binding and neutralizing activity against human VEGF-D, its *in vivo* anti-lymph node metastasis efficacy against VEGF-D-expressing tumors, and its possible indications for human cancer treatment.

2. Materials and Methods

2.1. Anti-VEGF-D antibody generation

Female BALB/c mice were immunized with recombinant VEGF-DΔNΔC, a polypeptide that contains amino acid residues 93 – 201 of human VEGF-D. After an increase in the serum titer was observed, splenocytes were prepared from the sacrificed mice and fused with myeloma cells. The resulting 5368 hybridoma cells were selected using a conventional HAT medium, IgG ELISA and binding activity to human VEGF-D.

Chimeric antibody genes were then constructed by linking the cDNAs of the variable regions in the antibody's heavy and light chains with the cDNAs of the constant regions from human IgG1 and kappa chains. The resultant chimeric antibodies were then heterologously expressed in HEK293 suspension culture and purified with protein A affinity chromatography and size-exclusion chromatography.

2.2. Binding assay for cVE199

For the binding assay, 96-well plates were coated with human VEGF-D (R&D Systems, USA) at 4°C overnight. After the plates were washed in 0.05% Tween20/PBS, they were incubated with Blocking One (Nacalai Tesque, Japan) for 1 h. The plates were then incubated with monoclonal antibody at the required dilutions. Bound monoclonal antibody was detected with an anti-human Ig-HRP (Life Technologies Japan, Japan). The assay was quantified by reading absorbance at 450 nm with an EnVision spectrophotometer (PerkinElmer, USA).

2.3. The inhibitory activity of cVE199 against the binding of VEGF-D to

VEGFR3

Stable human VEGFR-3-expressing CHO cells were aliquoted in a collagen type-I 96-well plate (Becton Dickinson, USA) and incubated for 2 days at 37°C. Following this, 2% FBS/HBSS containing 2.5 μg/mL of His-tagged recombinant protein (VEGF-D or VEGF-C) and/or monoclonal antibody was added, and the cells were then incubated for 1 h. After 3-times washes with 0.05% Tween20/PBS, the cells were incubated with polyHistidine-HRP MAb (R&D Systems) for 1 h. The assay was quantified by reading absorbance at 405/620 nm with a multi-well plate reader (Bio-Rad Laboratories, USA).

2.4. Immunoprecipitation

His-tagged human/mouse VEGF-D and His-tagged human VEGF-C were immunoprecipitated by cVE199 and Protein A agarose at 4°C overnight, followed by 3-times washes with PBS. The samples were subsequently analyzed by western blotting.

2.5. Neutralization assay with human lung lymphatic microvascular endothelial cells

Human lung lymphatic microvascular endothelial cells (HMVEC-LLy) were obtained from Takara Bio (Japan), and maintained according to the suppliers' instruction. MAZ-51 was purchased from Sigma-Aldrich Japan (Japan). For the assay, cells were aliquoted at 5×10^3 cells per well in a 96-well plate. After incubation for 16 h at 37°C, the cells were cultured in RPMI 1640 medium containing human VEGF-D and 0.1% FBS. Three days later, Cell Counting Kit-8 solution (Dojindo

Laboratories, Japan) was added. After the cells were incubated for several hours, absorbance at 450 nm was measured with an EnVision spectrophotometer (PerkinElmer).

2.6. Cell culture

Cell lines were obtained from the American Type Culture Collection (USA), the Deutsche Sammlung von Mikroorganismen und Zellkulturen (Germany), and Health Science Research Resources Bank (Japan). All cell lines were cultured according to the suppliers' instructions.

2.7. VEGF-D quantification by sandwich ELISA

All VEGF-D quantification by ELISA in this study was performed by the Quantikine Human VEGF-D ELISA kit (R&D Systems). For the screening of VEGF-D-expressing tumor cells, 100 μg of protein from each cell line was analyzed. For the detection of secreted VEGF-D, cells (5×10^5/well) were cultured in 6-well plates for 72 h in the condition medium. Following this, the supernatants were analyzed.

2.8. Gene expression analysis by Taqman

RNA was isolated from cells using the RNeasy Mini Kit (Qiagen), and cDNAs were synthesized using the High Capacity RNA-to-cDNA Kit (Applied Biosystems). For real-time PCR analysis, 40 ng of cDNA was used for each reaction. Detection of the human *VEGF-D* gene was performed using Taqman probe (Hs01128661_m1, Applied Biosystems). The expression level of each gene was quantified against the house-keeping gene *Gapdh* (402869, Applied Biosystems) in the same treatment.

Reactions were run on the 7900HT Fast Real-Time PCR system (Applied Biosystems), and the calculation of the delta Ct value was performed using the Sequence Detection System (SDS) software v2.3.

2.9. Western blotting

Western blotting was performed as described previously (Ono et al. 2012). The following primary antibodies were used: His-tag (MBL, Japan), VEGF-D (Santa Cruz Biotechnology, USA), VEGFR-2, VEGFR-3, pY1175-VEGFR-2 (Cell Signaling, USA), pY1063/1068-VEGFR-3 (Cell Applications, USA), and tubulin-alpha (AbD Serotec, UK). Signals were detected using ECL Plus (GE Healthcare, USA), followed by LAS-4000 (Fujifilm, Japan). Images were edited with MultiGauge (Fujifilm, Japan).

2.10. Animal care

All *in vivo* studies described here were conducted following the protocol approved by the Chugai Institutional Animal Care and Use Committee. All animal experiments were performed in accordance with the "Guidelines for the Accommodation and Care of Laboratory Animals" of Chugai Pharmaceutical Co. Ltd. All animals were housed in a pathogen-free environment under controlled conditions (temperature: 20–26°C, humidity: 40–70%, light-dark cycle: 12–12 h). Chlorinated water and irradiated food were provided *ad libitum*. The animals were allowed to acclimatize and recover from shipping-related stress for 1 week prior to the study. The health of the mice was monitored daily.

2.11. Mouse xenograft study

SK-N-DZ_luc cells (5×10^6 in HBSS with BD Matrigel™ matrix; BD Biosciences, USA) were subcutaneously inoculated in the right flanks of 6-week-old, female, CB-17 mice that had severe combined immunodeficiency (SCID; C.B-17/Icr-scid Jcl; Japan CLEA, Japan). After interperitoneal administration of luciferase substrate (65 mg/kg; VivoGloTM Luciferin, Promega, USA), the anaesthetized mice were imaged using an *in vivo* imaging system (NightOWL L983; Berthold Technologies GmbH & Co KG, Germany). Luciferase signals were visualized and quantified using WinLight32 (Berthold Technologies GmbH & Co KG) imaging software for NightOWL.

For the detection of lymph node metastasis, resected lymph nodes were sonicated and lysed with 100 μL of Cell Lysis Buffer (Cell Signaling) containing a complete protease inhibitor cocktail (Roche Diagnostics, Germany). The same amount of Bright-Glo luciferase assay system (Promega) was added. Assays were quantified by reading luminescence with an EnVision spectrophotometer (PerkinElmer).

For lymph vessel staining, 3 tumors from each treatment group were excised on day 14, weighed, and embedded in O.C.T compound (Tissuetek; Sakura Finetek Japan Co., Ltd., Japan), prior to being frozen in liquid nitrogen. Cryosections (5 μm) were fixed with ethanol and immunohistochemically stained for Lyve-1 using the Ventana automated immunostainer (Ventana Medical Systems Inc., USA). The following staining antibodies were used: polyclonal anti-mouse Lyve-1 antibody (RELIATech GmbH, Germany) and biotinized anti-rabbit-HRP antibody (Vector Laboratories, USA). The slides were counterstained with hematoxylin.

2.12. Immunohistochemical staining for VEGF-D

Twenty-nine tissue samples from neuroblastoma patients were obtained using a commercially available tumor microarray (US Biomax, Inc., USA) and tumor sections (TriStar Technology Group, LLC., USA). Following this, 10% formalin-fixed paraffin-embedded (FFPE) slides were stained with anti-VEGF-D antibody (sc-101584, Santa Cruz Biotechnology), using a Ventana automated immunostainer (Ventana Medical Systems, Inc.), according to the manufacturer's protocol. In brief, slides were pretreated with heat for 90 min by cell-conditioning solution 1 (Ventana Medical Systems, Inc.). The first antibody was incubated for 32 min at 37°C. Signals were visualized with ultraView Universal DAB detection kit (Ventana Medical Systems, Inc.).

To evaluate VEGF-D expression levels, the number of positively stained cells per 1000 tumor cells was counted. The expression was scored based on the percentage of positively stained cells. All cases were judged to be positive for VEGF-D when the proportion of immunoreactive tumor cells was greater than 30%.

2.13. Statistical analyses

All statistical tests in this study were performed using the Mann-Whitney U test. $P < 0.05$ was considered to be significant. Statistical analyses were performed using the SAS preclinical package (version 8.2; SAS Institute Inc., USA).

3. Results

3.1. cVE199, a human VEGF-D–specific monoclonal antibody

First, the author generated a monoclonal human mouse chimeric antibody against human VEGF-D, which was designated cVE199, as described in Materials and Methods.

The binding activity of cVE199 to human VEGF-D was determined by an antigen-coated ELISA (Fig. 1-1a). The binding specificity against human VEGF-D was evaluated by immunoprecipitation using His-tagged human VEGF-D, His-tagged mouse VEGF-D, and His-tagged human VEGF-C, the most closely related protein to VEGF-D. As shown in Fig. 1-1b, cVE199 specifically bound to human VEGF-D.

Next, the author investigated the inhibitory activity of cVE199 against the binding of human VEGF-D to VEGFR-3. The author found that cVE199 dose-dependently inhibited the binding of human VEGF-D to VEGFR-3 (Fig. 1-1c). Consistent with the binding specificity shown in Fig. 1-1b, cVE199 did not inhibit the binding of mouse VEGF-D or human VEGF-C to VEGFR-3 (Fig. 1-1d, e).

3.2. cVE199 neutralizes the biological activity of human VEGF-D

To evaluate the neutralizing activity of cVE199 against the biological activity of human VEGF-D, the author used human lymph endothelial cells derived from human lung tissues (HMVEC-Lly). HMVEC-Lly cells express VEGFR-3 (data not shown) and their proliferation was enhanced by VEGF-D. When HMVEC-Lly cells were incubated with cVE199, the VEGF-D-dependent growth of HMVEC-Lly was inhibited in a dose-dependent manner (Fig. 1-2a).

The author then determined how cVE199 alters VEGF-D-derived signal transduction in HMVEC-Lly cells. VEGF-D induced the phosphorylation of

VEGFR-2 and VEGFR-3, which was inhibited by cVE199, when used at the highest concentration (5 μg/mL). At lower concentrations, cVE199 inhibited VEGFR-3, but not VEGF-D-induced VEGFR-2 phosphorylation (Fig. 1-2b). These data suggested that cVE199 preferentially inhibited VEGF-D/VEGFR-3 signaling, thereby inhibiting VEGF-D-dependent proliferation. To confirm these data, the author used MAZ-51, a commercially available VEGFR-3 kinase inhibitor (Kirkin et al. 2001). MAZ-51 completely inhibited VEGF-D-dependent proliferation of HMVEC-Lly (Fig. 1-2c).

3.3. SK-N-DZ is a VEGF-D-expressing tumor cell line

Many reports suggested that VEGF-D in tumor originated from the tumor cells themselves (White et al. 2002, Nakamura et al. 2003, Yokoyama et al. 2003, Juttner et al. 2006, Liu et al. 2008, Thelen et al. 2008). Therefore, in order to evaluate cVE199 activity against tumor progression, the author investigated VEGF-D-expressing tumor cell lines. A VEGF-D ELISA using cell lysates was performed against 175 tumor cell lines. A neuroblastoma cell line, SK-N-DZ, expressed VEGF-D (Table 1-1).

To confirm VEGF-D expression in SK-N-DZ cells and to investigate the relationship between VEGF-D expression and neuroblastoma, 10 neuroblastoma cell lines, including SK-N-DZ, were analyzed in detail. The expression of *VEGF-D* mRNA was evaluated by real-time PCR. The author found that SK-N-DZ presented the highest *VEGF-D* mRNA expression among the 10 neuroblastoma cell lines, followed by KELLY and IMR-32 cells (Fig. 1-3a). Consistent with the mRNA expression patterns, VEGF-D precursor protein expression (about 50 kDa) was

strongly detected in SK-N-DZ cells and more weakly detected in KELLY and IMR-32 cells using western blot (Fig. 1-3b). The detection specificity in this assay was confirmed by using a VEGF-D siRNA (data not shown). Although these results were obtained by using tumor cell lysates, VEGF-D is a secreted protein and, thus, the author also assessed the presence of the secreted form of VEGF-D in the supernatant of the neuroblastoma cell lines using a VEGF-D ELISA. VEGF-D was detectable only in the supernatant of SK-N-DZ cells (Fig. 1-3c). These data indicate that the SK-N-DZ cell line is a VEGF-D-expressing tumor cell line.

The author further confirmed VEGF-D expression in SK-N-DZ xenograft tumors by VEGF-D immunohistochemistry (IHC). To do so, the author generated a HEK293 cell line stably expressing human VEGF-D (293-VEGF-D). VEGF-D expression in 293-VEGF-D was confirmed by VEGF-D ELISA (Fig. 1-4a). The specificity of the VEGF-D staining was confirmed by comparing the staining of 293-VEGF-D with that of parental HEK293 cells, (Fig. 1-4b). In addition, SH-SY5Y xenograft tumors were also used as negative controls for VEGF-D staining, because SH-SY5Y did not express VEGF-D in my *in vitro* analysis (Fig. 1-3b, c). As shown in Figure 1-5a, SK-N-DZ xenograft tumors stained for VEGF-D, while SH-SY5Y xenograft tumors were negative for VEGF-D. Furthermore, the author evaluated the status of lymph vessels in these xenograft tumors with a mLyve-1 IHC assay because VEGF-D is a lymphangiogenic factor. Consistent with the VEGF-D staining pattern, the SK-N-DZ xenograft tumors stained positive for mLyve-1, while SH-SY5Y xenograft tumors were negative for mLyve-1 (Fig. 1-5b).

3.4. cVE199 inhibited *in vivo* lymphatic metastasis of SK-N-DZ

The author next investigated the *in vivo* effect of cVE199 against lymphatic metastasis of SK-N-DZ cells in mice. To do so, the author generated a SK-N-DZ cell line stably expressing luciferase (SK-N-DZ-luc) in order to conduct bioimaging in mice (Fig. 1-6a). Compared to the SK-N-DZ parental cells, the SK-N-DZ-luc cells exhibited similar levels of VEGF-D expression *in vitro* (Fig. 1-6b). Furthermore, the *in vitro* proliferation of SK-N-DZ-luc cells did not differ from that of SK-N-DZ cells (Fig. 1-6c). In addition, the author evaluated VEGFR-2 and VEGFR-3 expression in SK-N-DZ-luc cells to consider the autocrine effect of VEGF-D. SK-N-DZ-luc cells did not express either VEGFR-2 or VEGFR-3 (Fig. 1-7).

Next, an *in vivo* efficacy study was performed by inoculating SK-N-DZ-luc cells into SCID mice and by a twice-weekly intravenous administration of 10 mg/kg cVE199 (n = 10). On the 14^{th} day after the first administration, a slight difference in the tumor size of SK-N-DZ-luc in the primary lesion was observed between the cVE199-injected mice and the vehicle-injected mice (Fig. 1-8a, b). In contrast, SK-N-DZ-luc cell metastasis into the ipsilateral lymph nodes (lymphatic metastasis) was significantly decreased by cVE199 injection on the 14^{th} day after the first administration ($p < 0.05$, Fig. 1-5c). The individual data shown in Fig. 1-8c (the amount of photons and the number of metastasized SK-N-DZ-luc cells) are presented in Fig. 1-9. In order to evaluate the association of lymph vessels with the reduction of metastasis into the lymph nodes, the author then analyzed lymph vessels in primary tumors using mLyve-1 IHC. As shown in Fig. 1-8d, the immunohistochemical signal for mLyve-1 in cVE199-injected xenograft tumors was much weaker than that in control xenograft samples. In contrast, the

immunohistochemical signal for mCD31 was not different between the 2 groups. This indicated that cVE199 did not affect blood vessels within the primary SK-N-DZ-luc tumors (Fig. 1-10). These data further indicate that cVE199 decreased SK-N-DZ-luc cell lymphatic metastasis by inhibiting lymph vessel formation.

3.5. Neuroblastoma is a potential indication for cVE199

Since only a neuroblastoma cell line, SK-N-DZ, abundantly expressed VEGF-D in my *in vitro* culture analysis, the author investigated VEGF-D expression in tumor tissues from patients with neuroblastoma. Twenty-nine commercially available neuroblastoma specimens were analyzed by IHC, as described in Materials and Methods. Using the criteria for VEGF-D immunohistochemical evaluation, VEGF-D-positive staining was detected in 11 cases (37.9%). Typical examples of VEGF-D-positive and VEGF-D-negative staining are presented in Fig. 1-11a and b respectively. These results indicate that some patients with neuroblastoma express VEGF-D.

4. Discussion

Lymphatic spread is an important clinical determinant in the prognosis of many cancers. Therefore, therapeutic modalities capable of inhibiting lymphatic spread should be beneficial for the treatment of many cancers. VEGF-D is implicated in lymphatic spread through the promotion of lymphangiogenesis in human cancers. In addition, high VEGF-D expression correlates with poor prognosis in many cancers. These findings suggest that an anti-VEGF-D antibody would be a promising agent for cancer treatment.

In this study, the author generated a novel anti-VEGF-D chimeric monoclonal antibody, cVE199, which specifically binds to and neutralizes human VEGF-D. Using HMVEC-Lly cells, the author showed that cVE199 preferentially inhibited the VEGF-D/VEGFR-3 signaling pathway rather than the VEGF-D/VEGFR-2 signaling pathway (Fig. 1-2b). A recent study showed that N-terminal residues of VEGF-D are important for VEGF-D binding and activation of VEGFR-3, but not for that of VEGFR-2 (Leppanen et al. 2011). This finding suggested that cVE199 binds to N-terminal residues of VEGF-D, thereby preferentially inhibiting VEGF-D/VEGFR-3 signaling.

In a xenograft study to evaluate the *in vivo* effect of cVE199, the author used SK-N-DZ cells that express VEGF-D endogenously, though previous studies used VEGF-D-transfected cell lines. This approach is important because it has a higher clinical relevance compared to overexpression experiments. My results indicated that cVE199 significantly decreased lymph node metastasis of SK-N-DZ cells with reduction of lymphangiogenesis, strongly supporting previously published conclusions drawn from VEGF-D overexpressing *in vivo* studies. These reports

largely attributed the metastatic action of VEGF-D to an induction of lymphangiogenesis. For instance, VEGF-D stimulated lymphangiogenesis when the molecule was overexpressed in the skin keratinocytes (Veikkola et al. 2001). It promoted the development of lymphatics and lymph node metastasis when overexpressed in tumors (Stacker et al. 2001, Thelen et al. 2008).

In this study, cVE199 did not alter blood vessels in the primary SK-N-DZ-luc xenograft tumors. Although the VEGF-D/VEGFR-3 pathway is known to play a role not only in tumor lymphangiogenesis, but also in pathological angiogenesis, the VEGF-A/VEGFR-2 signal is known as the predominant regulator of physiological and tumor angiogenesis (Bergers and Benjamin 2003). The author found that SK-N-DZ-luc cells expressed VEGF-A (Fig. 1-12). In addition, VEGFR-3 kinase inhibitor or VEGFR3-Ig, a potent inhibitor of VEGF-C/VEGF-D signaling, did not always affect tumor angiogenesis (Wong et al. 2005, Yashiro et al. 2009). These data suggest that the contribution of VEGF-D/VEGFR-3 signaling to tumor angiogenesis is affected by *in vivo* circumstances such as VEGF-A expression. Furthermore, these findings might explain the reason for the ineffectiveness of cVE199 on tumor angiogenesis in SK-N-DZ-luc xenograft tumors.

Because cVE199 did not affect tumor growth (Fig. 1-8a, b) or angiogenesis (Fig. 1-10), it seems that cVE199 inhibits lymph node metastasis of SK-N-DZ-luc cells by inhibiting lymphangiogenesis. Thus, my findings also support previously published data, which showed that formation of a dense lymphatic network that facilitates metastatic tumor spread by increasing the likelihood that tumor cells will leave the primary tumor site and invade the lymphatics (Detmar and Hirakawa 2002).

One of the most important findings was that cVE199 inhibits lymphatic metastasis

in an experimental neuroblastoma model (Fig. 1-8) and that VEGF-D was expressed in some human neuroblastomas (Fig. 1-11), implicating VEGF-D in neuroblastoma lymphatic metastasis. These findings further suggest cVE199 as a possible therapeutic antibody for neuroblastoma. Although many lower-stage neuroblastomas regress completely or differentiate into benign ganglioneuroblastoma without treatment, metastatic neuroblastoma (stage IV) in children over 1 year of age is lethal for most patients despite aggressive multimodality therapy (Brodeur 2003, Maris et al. 2007, Maris 2010, Modak and Cheung 2010). Therefore, new therapeutic agents for neuroblastoma are still necessary and my finding that cVE199 has potential as a therapeutic antibody for neuroblastoma is of significance.

In conclusion, the results of the present study implicate VEGF-D in the promotion of neuroblastoma lymphatic metastasis and identify cVE199 as a potential therapeutic antibody against neuroblastoma to prevent this process.

5. Tables

Table 1-1. Screening of VEGF-D expressing tumor cells

Tissue	Cell line	VEGF-D (pg/mg protein)
Blood	CMK-11-5	§
	THP-1	§
	L-363	§
	SR	§
	ARH-77	§
	F-36P	§
	Kasumi-1	§
	MOLM-13	§
	MV4-11	§
	SKM-1	§
Bone Marrow	KHM-1B	§
	KMM-1	§
	KMS-26	§
	KMS-11	§
	KMS-12-BM	§
	KMS-12-PE	§
	KMS-20	§
	KMS-21 BM	§
	KMS-26	§
	KMS-28 BM	§
	KMS-34	§
	LP-1	§
	OPM-2	§
Breast	MCF7	§
	MDA-MB-231	§
	MDA-MB-468	§
	COLO-824	§
	MDA-MB-453	§
	BT-474	§
	BT-483	§
	HCC1395	§
	HCC1599	§
	HCC-1937	§
	HCC38	§
	JIMT-1	§
	MFM-223	§
	T-47D	§
	ZR-75-1	§
	HCC-1806	§
Colon	COLO 201	§
	COLO205	§
	COLO320DM	§
	DLD-1	§
	HCT15	§
	HCT-8	§
	HT-29	§
	LoVo	§
	LS174T	§
	SW1417	§
	SW1116	§
	SW403	§
	SW480	§
	SW620	§
	SW948	§
	WiDr	§
	HCT116	§
	RKO	§
	T84	§
Neuron	SH-SY5Y	§
	SK-N-DZ	**853**
	SK-N-SH	§
Lung	A549	§
	ABC-1	§
	Calu-3	§
	HCC-827	§
	NCI-H1437	§
	NCI-H1650	§
	NCI-H1666	§
	NCI-H1703	§
	NCI-H1755	§
	NCI-H1781	§
	NCI-H1793	§
	NCI-H1838	§
	NCI-H1975	§
	NCI-H1993	§
	NCI-H2009	§
	NCI-H2023	§
	NCI-H2029	§
	NCI-H2030	§
	NCI-H2122	§
	NCI-H2228	§
	NCI-H23	§
	NCI-H2347	§
	NCI-H441	§
	NCI-H508	§
	NCI-H522	§
	NCI-H716	§
	NCI-H838	§
	Calu-6	§
	NCI-H596	§
	NCI-H1299	§
	NCI-H460	§
	NCI-H661	§
	PC-13	§
	NCI-H1048	§
	NCI-H146	§
	NCI-H187	§
	NCI-H2081	§
	NCI-H209	§
	NCI-H345	§
	NCI-H446	§
	NCI-H526	§
	NCI-H69	§
	NCI-H82	§
	SCLC-21H	§
	Calu-1	§
	NCI-H2170	§
	NCI-H226	§
	NCI-H520	§
	SK-MES-1	§
	NCI-H929	§
Kidney	786-O	§
	769-P	§
	Caki-1	§
	Caki-2	§
	ACHN	§
Pancreas	Hs 38.T	§
	HPAF-II	§
	AsPC-1	§
	BxPC-3	§
	Capan-1	§
	Capan-2	§
	CFPAC-1	§
	SU.86.86	§
	Hs766T	§
	HUP-T4	§
	MIA PaCa-2	§
	PANC-1	§
	YAPC	§
Prostate	PC3	§
	22Rv1	§
	DU145	§
	WERI-Rb-1	§
Skin	HMCB	§
	MDA-MB-435S	§
	SK-MEL-5	§
	SK-MEL-1	§
	SK-MEL-2	§
	SK-MEL-28	§
	SK-MEL-30	§
	C32	§
	AGS	§
Stomach	KATO III	§
	MKN-1	§
	MKN-28	§
	MKN-45	§
	MKN-74	§
	NCI-N87	§
	NUGC-3	§
	NUGC-4	§
	SCH	§
	SNU-16	§
	SNU-5	§
Bladder	5637	§
	BFTC-905	§
	HT-1197	§
	HT-1376	§
	RT4	§
	SW780	§
	T24	§
	TCCSUP	§
	UM-UC-3	§
Liver	SK-HEP-1	§
	Hep 3B	§
	Hep G2	§
	HuH-7	§
	PLC/PRF/5	§
Ovary	Caov-4	§
	COLO-704	§
	ES-2	§
	OVCAR-3	§
	SK-OV-3	§
	PA-1	§

NOTE: VEGF-D ELISA assay was performed with various cell lysate as described in Materials and Methods.
§ indicates under the detection in ELISA assay

6. Figures

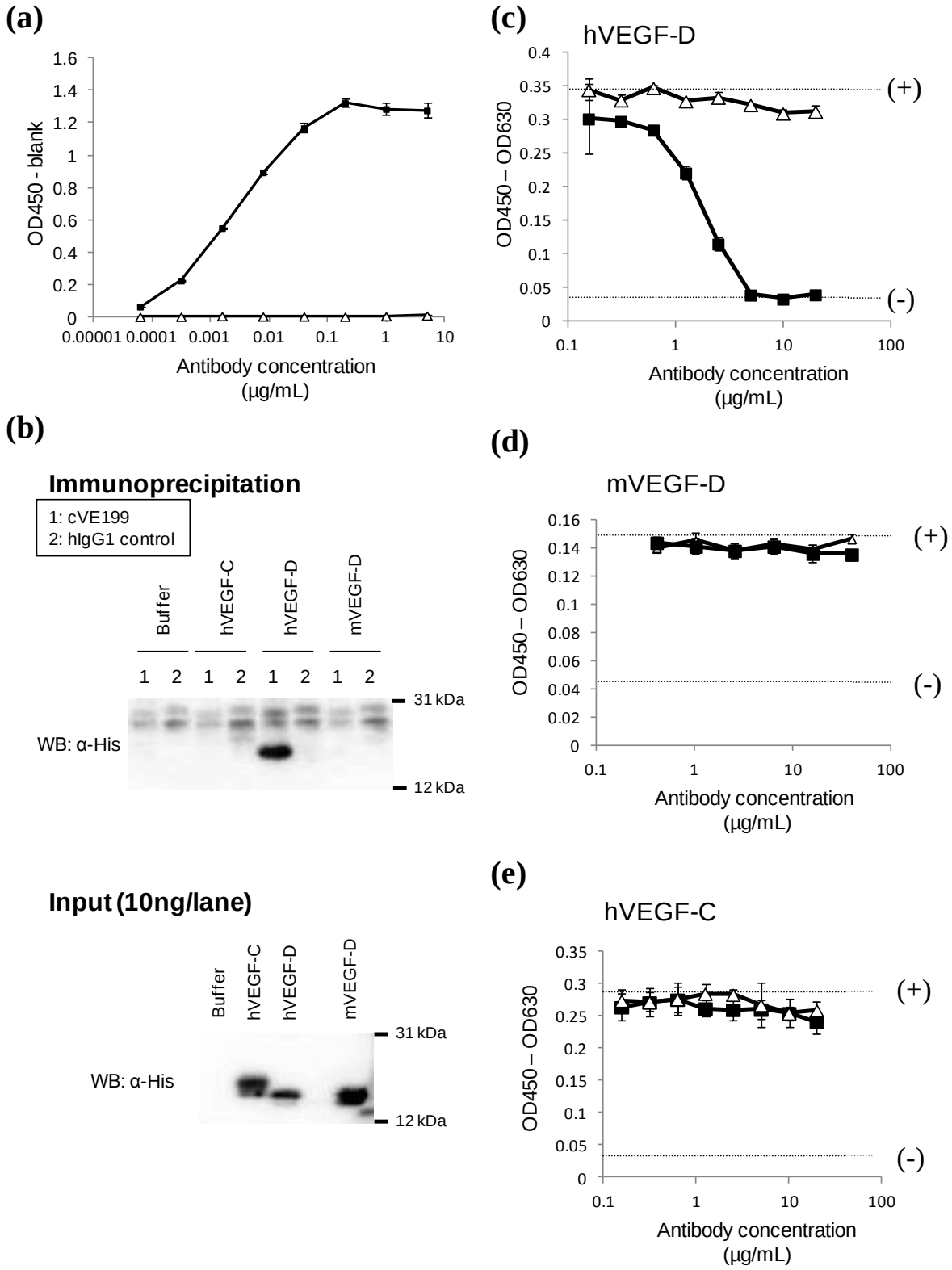
(a)
OD450 - blank
Antibody concentration (μg/mL)
(b)
Immunoprecipitation
1: cVE199
2: hIgG1 control
Buffer
hVEGF-C
hVEGF-D
mVEGF-D
WB: α-His
31 kDa
12 kDa
Input (10ng/lane)
(c)
hVEGF-D
OD450 – OD630
(+)
(-)
(d)
mVEGF-D
(e)
hVEGF-C

Fig. 1-1. Reaction specificity of cVE199 against rhVEGF-D.

(a) The binding activity of cVE199 to rhVEGF-D was measured by an ELISA. The various concentrations of cVE199 (■) and hIgG1 control (△) were reacted to plated hVEGF-D. Binding was detected by HRP-labeled anti-human IgG. (b) The binding specificity of cVE199 to hVEGF-D was evaluated by the immunoprecipitation as described in Materials and Methods. (c–e) The inhibitory activity of cVE199 against the binding of (c) hVEGF-D, (d) mVEGF-D, and (e) hVEGF-C to VEGFR3 was measured using a cell-based assay. His-tagged protein was incubated with VEGFR3 stably expressing CHO cells, in the presence or absence of various concentrations of cVE199 (■) and hIgG1 control (△). Binding was detected by polyHistidine-HRP MAb. The absorbance when 1.25 or 0 μg/mL of recombinant protein was added with no antibody is indicated by the (+) or (-) dotted lines, respectively. Points indicate the mean ± SD (n = 3).

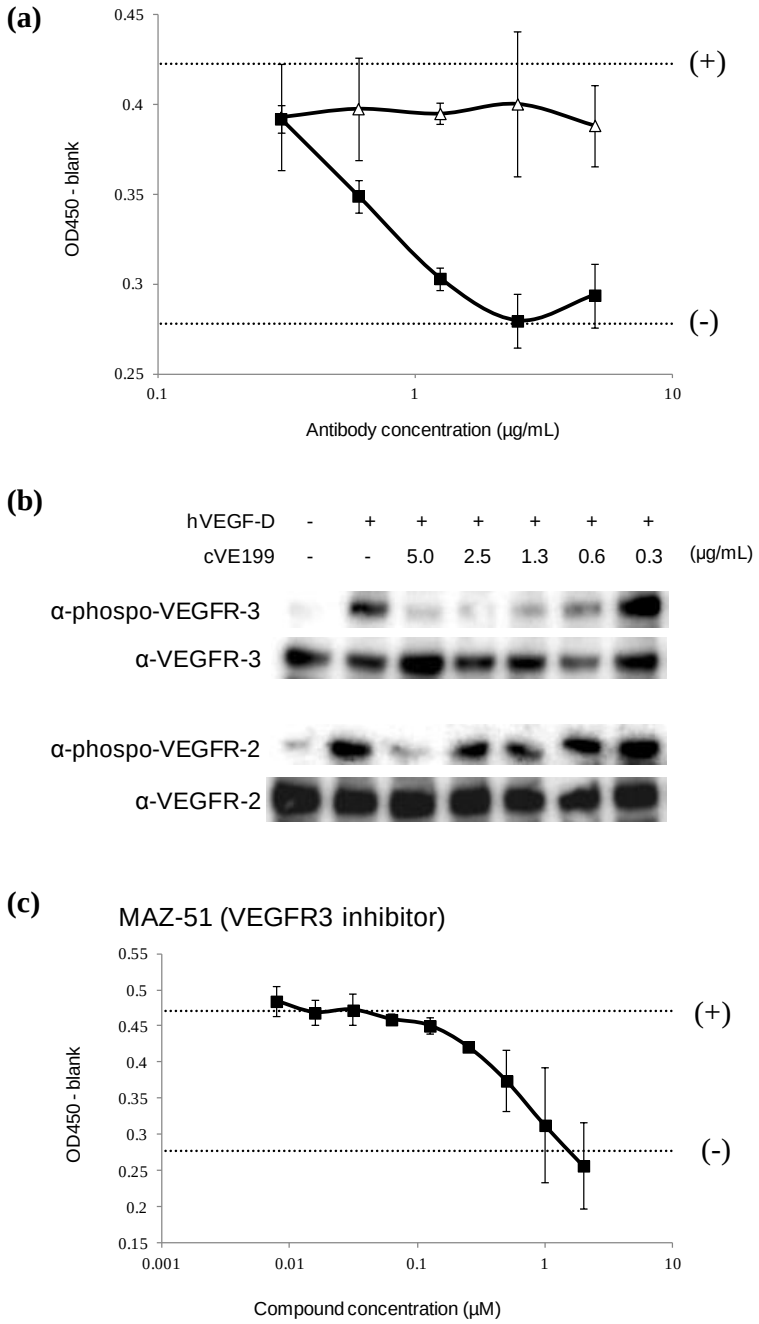

Fig. 1-2. Neutralization activity of cVE199 against rhVEGF-D.

The neutralization activity of cVE199 for VEGF-D was measured using HMVEC-Lly cells. (a) A total of 500 ng/mL of VEGF-D was pre-incubated with serially diluted cVE199 (■) and hIgG1 control (△) for 15 min at 37°C, and added to HMVEC-Lly cells for 72 h. The number of living cells was then measured using a Cell Counting Kit-8 solution. The cell number when 500 or 0 ng/mL of VEGF-D was added with no antibody is indicated by the (+) or (-) dotted line, respectively. (b) HMVEC-Lly cells were incubated with cVE199 and VEGF-D. After 10 min, the cells were harvested and analyzed by western blotting with phospho-VEGFR-2 and phospho-VEGFR-3 antibodies. (c) MAZ-51 was used instead of cVE199. Assay was conducted by the same method as (a). All points indicate the mean ± SD (n = 3).

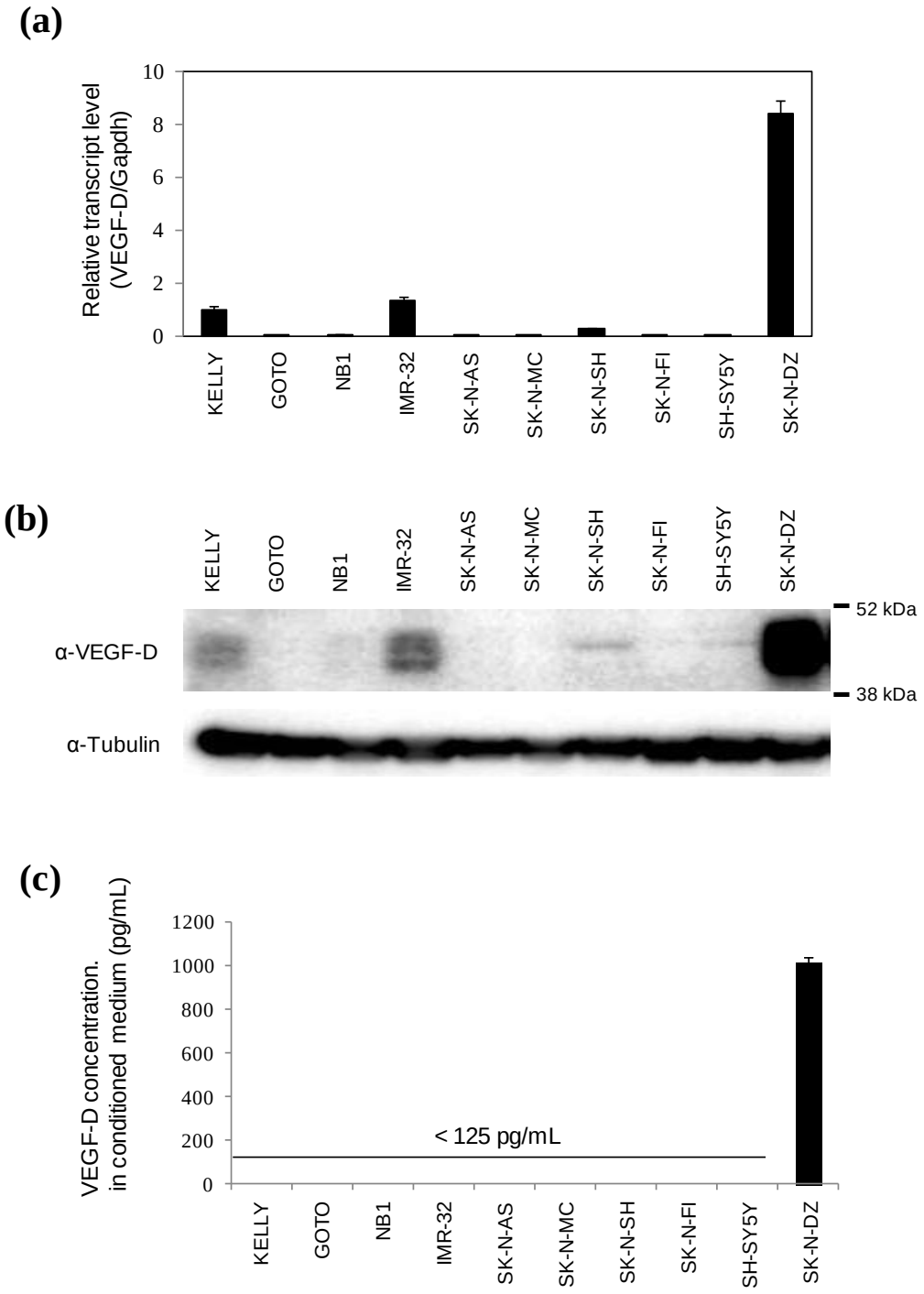

Fig. 1-3. Analysis of VEGF-D expression in neuroblastoma cell lines.

(a) VEGF-D mRNA expression in 10 neuroblastoma cell lines was analyzed by the Taqman assay (n = 3 for each cell line). Data were normalized to Gapdh. (b) Expression of VEGF-D protein in 10 neuroblastoma cell lines was analyzed by western blot using anti-VEGF-D antibody. (c) Each cell line was cultured for 72 h in the condition medium. The VEGF-D concentration in the medium was quantified using the VEGF-D ELISA kit (n = 3 for each cell line). All values are expressed as the mean ± SD.

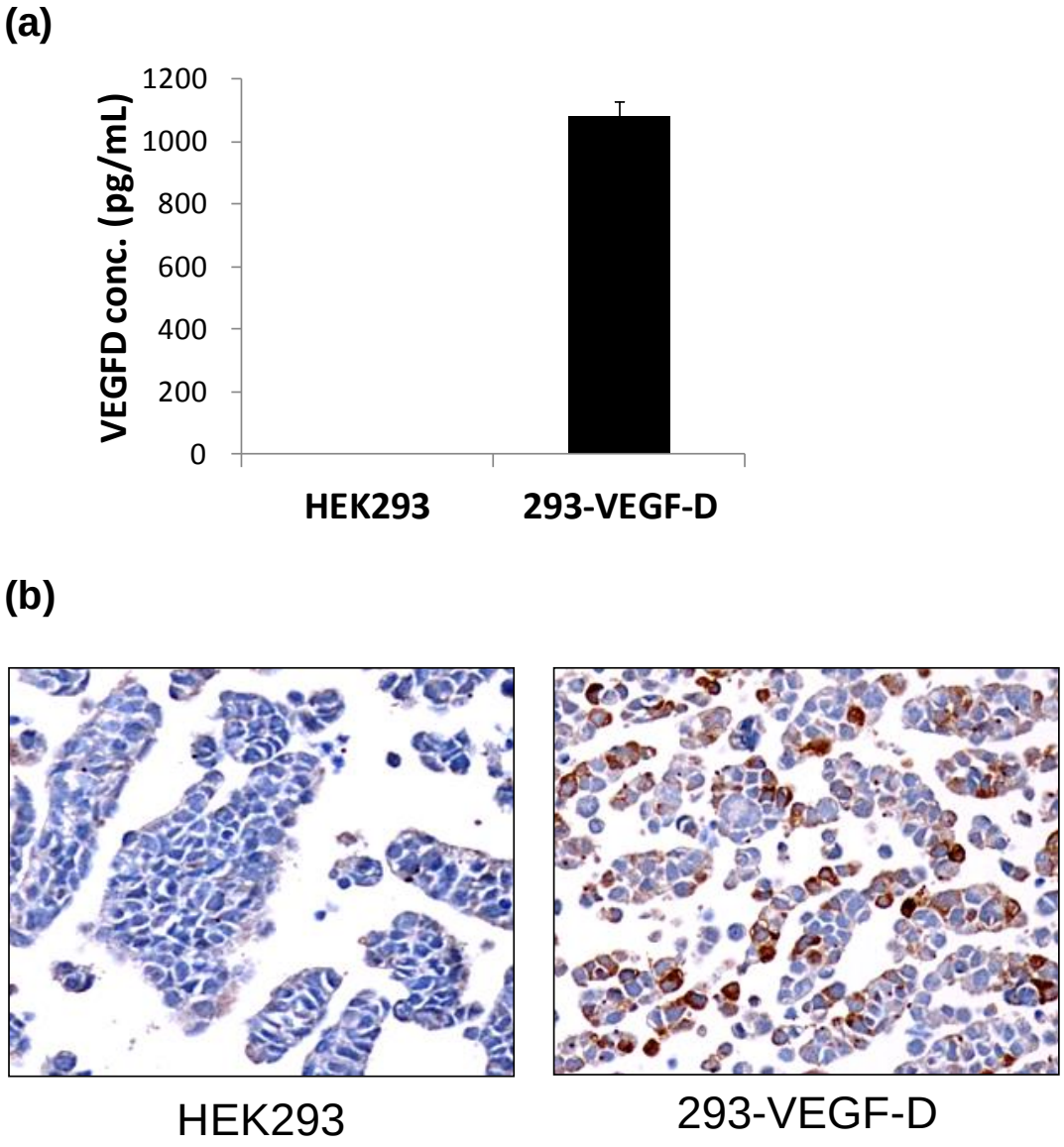

Fig. 1-4. Evaluation of the specificity of VEGF-D immunohistochemical analysis.
(a) VEGF-D expressing HEK293 cells (293-VEGF-D) were generated by lectroporation with the human VEGF-D expression vector. VEGF-D expression was confirmed by Quantikine Human VEGF-D ELISA kit (n = 3 for each cell line). (b) Specificity of immunohistochemical analysis for VEGF-D was evaluated by staining comparison with HEK293 and 293-VEGF-D. FFPE slides were stained with anti-VEGF-D antibody by a Ventana automated immunostainner.

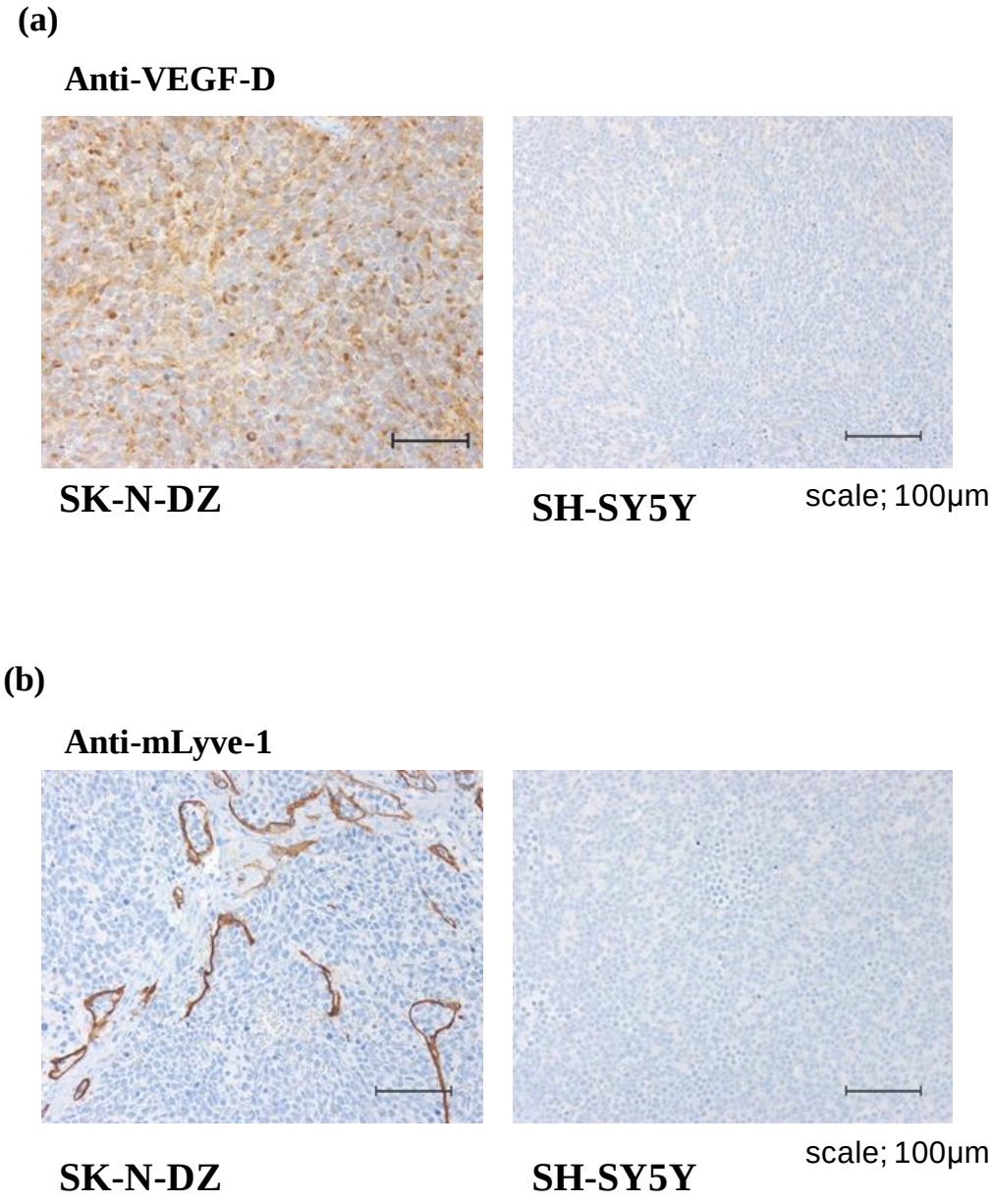

Fig. 1-5. Analysis of VEGF-D expression in neuroblastoma xenograft.
Expression of VEGF-D in neuroblastoma xenograft was evaluated by immunohistochemistry with anti-VEGF-D antibody. FFPE slides were stained by a Ventana automated immunostainer. (a) SK-N-DZ showed an immunohistochemical signal for VEGF-D (b) and SH-SY5Y showed immunonegativity to VEGF-D.

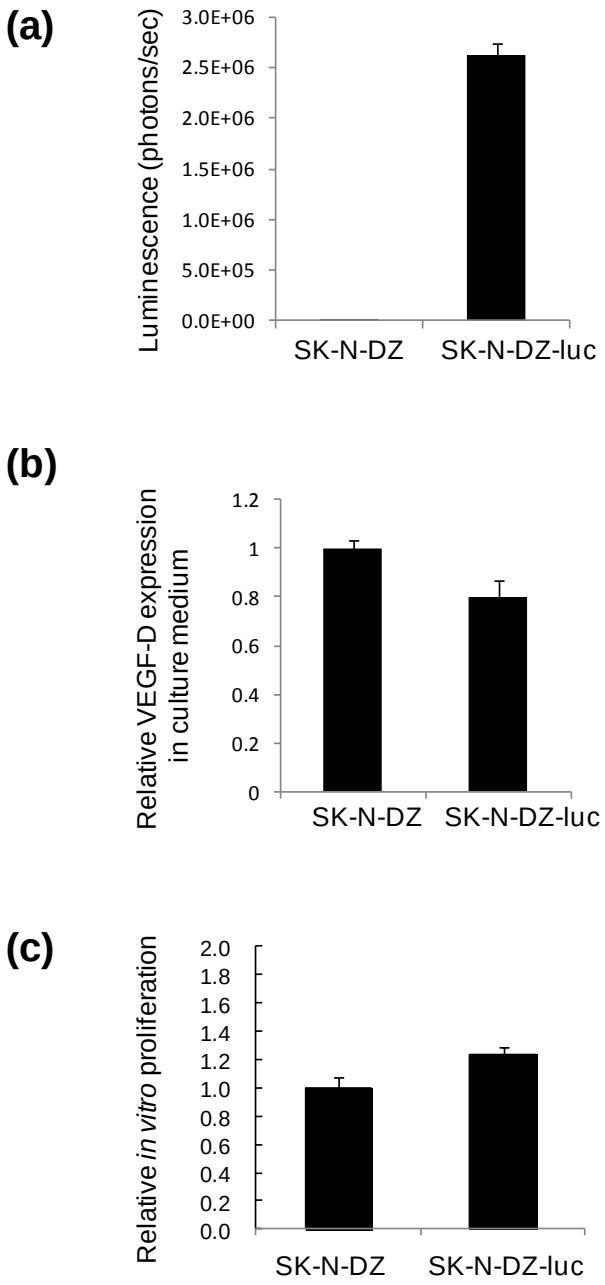

Fig. 1-6. Comparison of profile between SK-N-DZ and SK-N-DZ-luc cells.

(a) SK-N-DZ-luc was generated by infection of lentivirus with luciferase expression region. Luciferase activity was confirmed by Bright-Glo luciferase assay system (n = 3 for each cell line). (b) Comparison of secreted VEGF-D level between SK-N-DZ and SK-N-DZ-luc cells was analyzed by Quantikine Human VEGF-D ELISA kit (n = 3 for each cell line). (c) Comparison of *in vitro* proliferation ability between SK-N-DZ and SK-N-DZ-luc cells was quantified by Cell Count Kit (n = 3 for each cell line). All values are expressed as the mean ± SD.

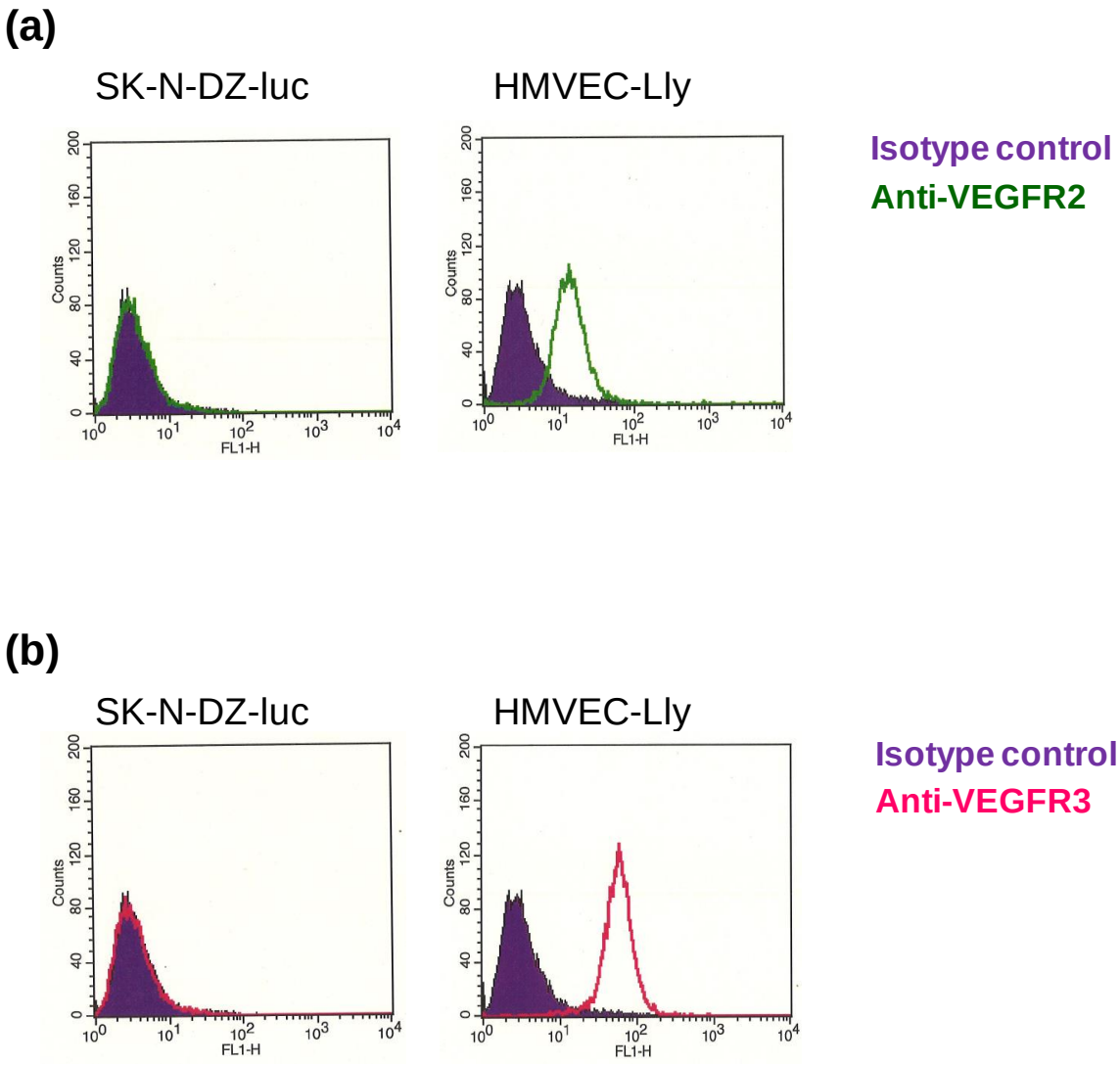

Fig. 1-7. Expression of VEGFR-2 and VEGFR-3 in SK-N-DZ-luc cells.

(a) VEGFR-2 and (b) VEGFR-3 expression on cell surface were analyzed by FACS with anti-VEGFR-2 and VEGFR-3 antibody (R&D systems). HMVEC-Lly was used as a positive control cell.

(a)

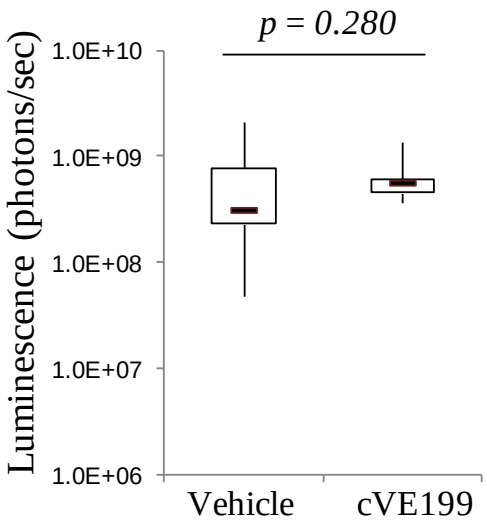
Tumor volume (primary site)
p = 0.280
Luminescence (photons/sec)
1.0E+10
1.0E+09
1.0E+08
1.0E+07
1.0E+06
Vehicle
cVE199

(b)

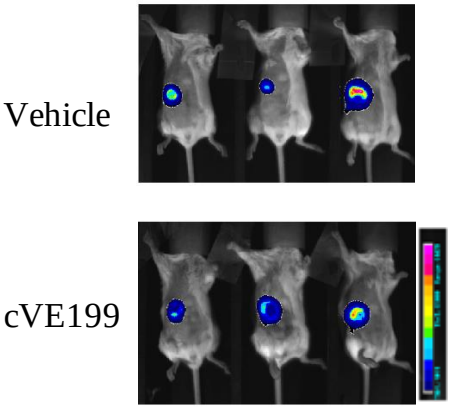
Vehicle
cVE199

(c)

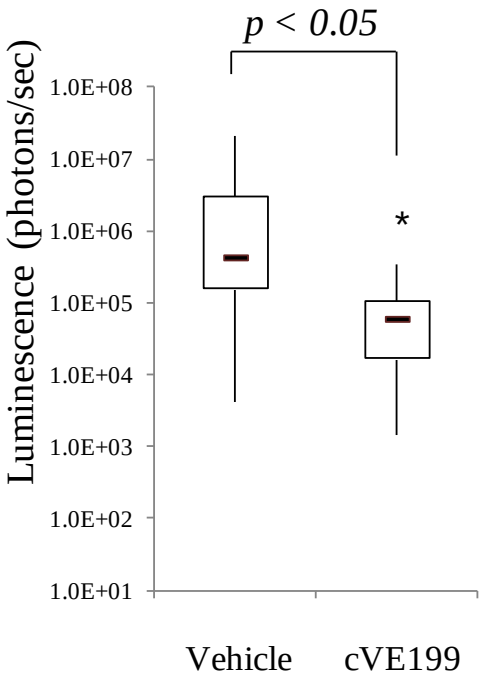
Tumors in lymph nodes
p < 0.05
Luminescence (photons/sec)
1.0E+08
1.0E+07
1.0E+06
1.0E+05
1.0E+04
1.0E+03
1.0E+02
1.0E+01
*
Vehicle
cVE199

(d)

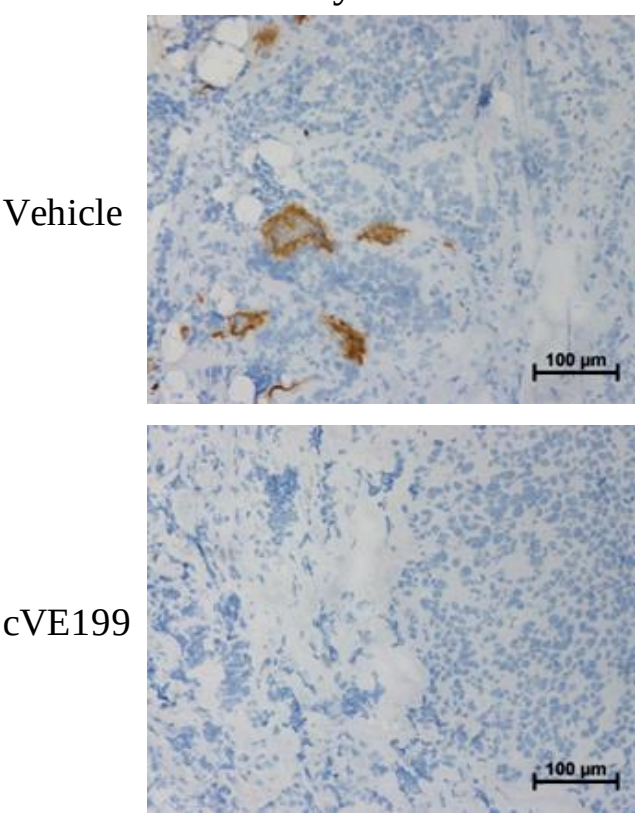
Anti- mLyve-1
Vehicle
cVE199
100 μm
100 μm

Fig. 1-8. *In vivo* effect of cVE199 against VEGF-D expressing neuroblastoma model. (a and b) Antitumor effect of cVE199 against SK-N-DZ primary lesion was evaluated by bioimaging technique. Mice bearing SK-N-DZ were administered with 10 mg/kg of cVE199 at biw regimen for 2 weeks. Tumor size was measured by administration of luciferase substrate and detection of the photons. Data are shown by a box-and-whisker plot. Statistical tests were performed using the Wilcoxon test. (c) Anti-metastasis activity of cVE199 against SK-N-DZ was evaluated by detection of photons from lysed lymph nodes. Data are shown by a box-and-whisker plot. Statistical tests were performed using the Wilcoxon test. (d) The presence of lymph vessels in the primary tumors of SK-N-DZ was analyzed by mLyve-1 immunostaining. FFPE slides were stained with an anti-mouse Lyve-1 antibody using a Ventana automated immunostainer.

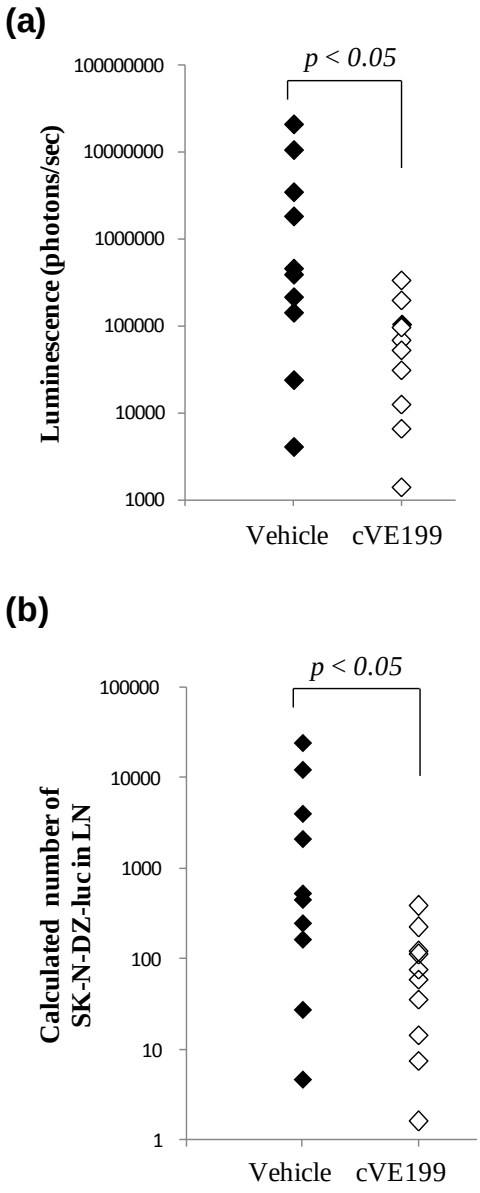

Fig. 1-9. Plot of photons and SK-N-DZ-luc number in each mouse shown in Fig. 1-8.

(a) The amount of photons in each mouse shown in Fig. 5c was plotted. (b) The number of SK-N-DZ-luc cells in each mouse shown in Fig. 5c was plotted. This cell number was calculated based on the result in Fig. S2a showing the relationship between the number of SK-N-DZ-luc and photons. All statistical tests were performed using the Wilcoxon test.

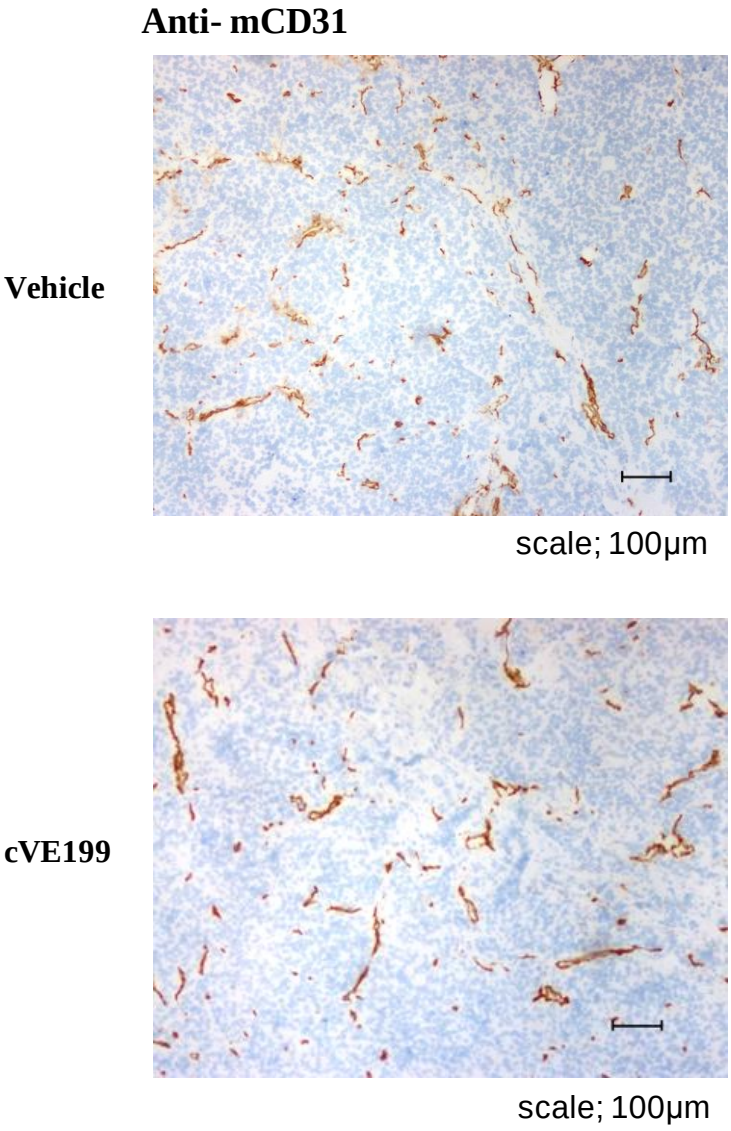

Fig. 1-10. Immunohistochemical analysis of mCD31 in SK-N-DZ-luc xenograft.

The presence of blood vessels in the primary tumors of SK-N-DZ was analyzed by CD31 immunostaining. FFPE slides were stained with an anti-mouse CD31 antibody (BD Biosciences) using a Ventana automated immunostainer.

VEGF-D positive

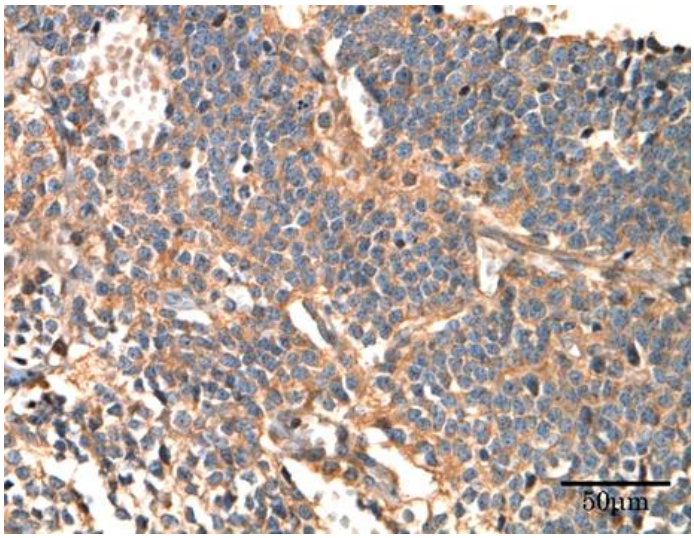

VEGF-D negative

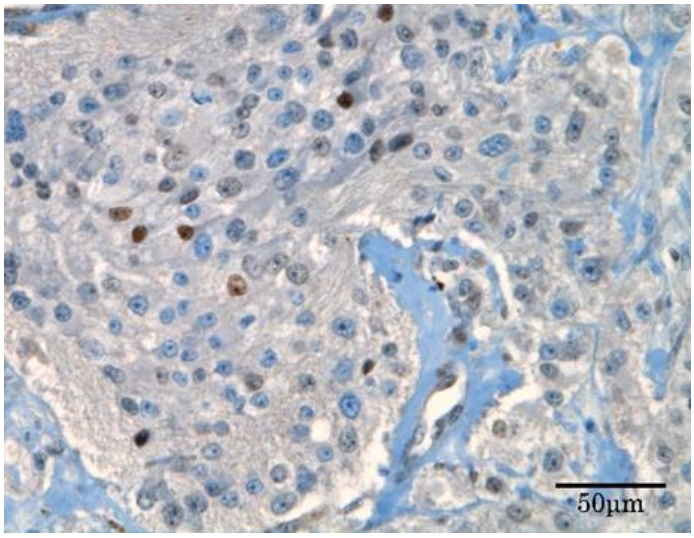

Fig. 1-11. Immunohistochemical analysis of VEGF-D in neuroblastomas.

Expression of VEGF-D in neuroblastoma specimens was evaluated by immunohistochemistry with anti-VEGF-D antibody. FFPE slides were stained by a Ventana automated immunostainer. According to the criteria for VEGF-D immunohistochemical evaluations as described in Materials and Methods, (a) tumor cells showed immunohistochemical signal for VEGF-D and (b) the tumor cells showed immunonegativity to VEGF-D.

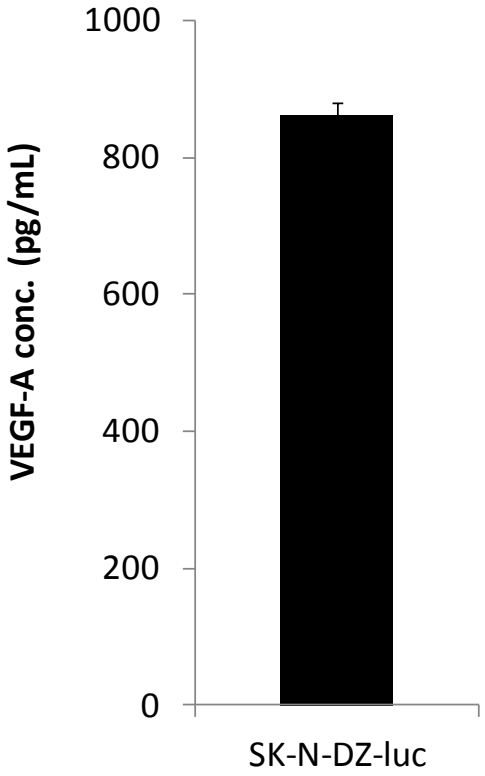

Fig. 1-12. Expression of VEGF-A in SK-N-DZ-luc cells.

Secreted VEGF-A level in SK-N-DZ-luc cells was analyzed by Quantikine Human VEGF-A ELISA kit (R&D systems). Assay was performed by n = 3. All values are expressed as the mean ± SD.

Chapter II: Blockade of CXCR4 by CF172 Inhibits Rhabdomyosarcoma Metastasis

1. Introduction

Rhabdomyosarcoma is the most common soft tissue sarcoma reported in children. During the last 30 years, the introduction of multimodal therapy has significantly improved cancer survival, with a cure rate of approximately 70% for patients exhibiting localized disease. Unfortunately, at least 15% of children with rhabdomyosarcoma exhibit metastatic disease and the prognosis for metastatic rhabdomyosarcoma has not improved significantly in the last 15 years, with an overall cure rate below 30% (Koscielniak et al. 1992, Crist et al. 2001, Breneman et al. 2003, Stevens et al. 2005, Oberlin et al. 2008, Malempati and Hawkins 2012). Therefore, there is a critical need to develop therapeutics to treat metastatic rhabdomyosarcoma.

Organ-specific patterns of metastasis associated with different tumor types were first described by Paget's "seed-and-soil" hypothesis (Paget 1989). This hypothesis states that tumor cells may form metastases at sites that (a) chemoattract and arrest tumor cells by locally secreted factors and (b) provide a favorable microenvironment for tumor cell survival and growth (Kucia et al. 2004). Chemokines are small pro-inflammatory chemoattractant proteins that bind to G-protein coupled receptors present on the cell surface of target cells. These chemokines are major regulators of cell trafficking, survival, and growth (Rossi and Zlotnik 2000, Balkwill 2004, Strahm et al. 2008). The chemokine, stromal cell-derived factor 1 (SDF1), and its receptor, CXC chemokine receptor-4 (CXCR4), play a unique role in homing and migration

of hematopoietic and lymphopoietic cells (Kucia et al. 2004, Strahm et al. 2008). In addition, studies suggested that CXCR4 may be involved in the promotion of metastatic potential in multiple tumor types, by activating migration and homing of tumors (Muller et al. 2001, Burger 2006, Oda et al. 2007, Akashi et al. 2008, Joyce and Pollard 2009). Moreover, results of a recently published study indicated that high levels of CXCR4 expression in rhabdomyosarcoma correlated with metastatic potential and poor prognosis (Diomedi-Camassei et al. 2008). Therefore, blocking CXCR4 would be a promising approach in the treatment of metastatic rhabdomyosarcoma.

To explore this possibility, the author generated a novel anti-CXCR4 monoclonal antibody, CF172, and investigated its *in vitro* binding and neutralizing activity against human CXCR4 and its anti-metastatic efficacy against rhabdomyosarcoma cell lines.

2. Materials and Methods

2.1. Anti-CXCR4 antibody generation

Female Balb/c mice were immunized with CXCR4-stably expressed Ba/F3 cells. After an increase was observed in the serum titer of the anti-CXCR4 antibody, splenocytes were prepared from the sacrificed mice and fused with myeloma cells. The resulting 51656 hybridoma cells were selected using a conventional HAT medium, IgG ELISA and binding activity to human CXCR4.

Anti-CXCR4 antibody was typically produced from the culture of hybridoma cells, followed by purification with protein A affinity chromatography and subsequent size-exclusion chromatography.

2.2. Flow cytometry

The binding activity of CF172 for CXCR4 expressed on cell surfaces was examined by flow cytometry. Cells were stained on ice for 30 min with either CF172 or control mouse IgG2b (R&D Systems, USA). Becton Dickinson Stained cells were then analyzed using a FACSCalibur cell analyzer (Becton Dickinson).

2.3. Neutralization assay

Neutralization activity against CXCR4 was evaluated using the Tango CXCR4-bla U2OS cell-based assay system (Invitrogen, USA). For the assay, serially diluted antibody was pre-incubated with Tango CXCR4-bla U2OS for 30 min at 37°C. SDF1 (4 nM) was added to the cells, which were subsequently incubated for 5 h at 37°C. Cells were then loaded with LiveBLAzer FRET B/G substrate (Invitrogen) for 2 h at room temperature. Fluorescence spectra were acquired at 460 nm and 530 nm

(excitation wavelength 409 nm), using an EnVision Multilabel Plate Reader (PerkinElmer, USA).

For the neutralization assay against CXCR2, a PathHunter eXpress β-Arrestin GPCR assay system was used (DiscoveRx, USA). PathHunter CHO-K1 CXCR2 cells were incubated overnight at 37°C followed by 90 min incubation in the presence of CXCL8 (1.25 nM) and serially diluted antibody, followed by 1 h incubation with PathHunter detection reagent. Plates were then analyzed for a chemiluminescent signal using the EnVision Multilabel Plate Reader (PerkinElmer).

2.4. Cell cultures

SJCRH30, A-204 and A-673 were obtained from the American Type Culture Collection (USA). RD was purchased from DS Pharma Biomedical Co., Ltd (Japan). RH30 cells were obtained from the Deutsche Sammlung von Mikroorganismen und Zellkulturen (Germany). All cell lines were cultured according to the suppliers' instructions.

2.5. cAMP ELISA

SJCRH30 cells were grown as confluent monolayers in a 96-well plate. Before stimulation, cells were incubated for 30 min with monoclonal antibody and 1 mM IBMX (Sigma-Aldrich Japan, Japan). Cells were stimulated with 100 nM SDF1 (R&D systems) diluted in HBSS/IBMX for 10 min, after which they were incubated for an additional 10 min with 25 μM forskolin (Sigma-Aldrich Japan) to stimulate cAMP production. Then, cells were washed 2 times in ice-cold HBSS/IBMX and solubilized, and cAMP was assayed using the cAMP Parameter Assay Kit (R&D

systems).

2.6. Migration assay

Both CIM-Plate and the xCELLigence System RTCA DP analyzer (Roche Diagnostics, Germany) were used to monitor real-time migrations. The xCELLigence system is an electrical impedance-based system that allows for real-time cell monitoring (Ke et al. 2011). For this assay, 4×10^4 cells with antibodies, in growth medium, were seeded into the upper chamber of a CIM-Plate. The upper chamber was then placed on the lower chamber of the CIM-Plate which contained 10 nM SDF1. Cell migration was monitored for up to 7 h. Data were analyzed using RTCA software (Roche Diagnostics).

2.7. Western blotting

Western blotting was performed as described previously (Kashima et al. 2012). The following primary antibodies were used: anti-CXCR4 (Sigma-Aldrich Japan, Japan) and anti-tubulin-alpha (AbD Serotec, UK). Signals were detected using Chemi-Lumi One Super (Nacalai Tesque, Kyoto, Japan) with imaging on an LAS-4000 systems (Fujifilm, Japan). Images were edited with MultiGauge (Fujifilm).

2.8. Animal care

All *in vivo* studies described here were conducted following a protocol approved by the Chugai Institutional Animal Care and Use Committee. All animal experiments were performed in accordance with the "Guidelines for the Accommodation and Care of Laboratory Animals" of Chugai Pharmaceutical Co. Ltd. All animals were housed in a pathogen-free environment under controlled conditions (temperature, 20–26°C;

humidity, 40–70%; light-dark cycle, 12–12 h). Chlorinated water and irradiated food were provided *ad libitum*. The animals were allowed to acclimatize and recover from shipping-related stress for 1 week prior to the study. The health of the mice was monitored daily.

2.9. Mouse xenograft study for peritoneal metastasis

SJCRH30-luc cells (2×10^6 in HBSS) were intraperitoneally injected into nude mice (CAnN.Cg-Foxn1<nu>/CrlCrlj nu/nu, Charles River Japan). On the same day of SJCRH30-luc inoculation, 25 mg/kg CF172 was intravenously injected in a single shot. On day 5 after interperitoneal administration of luciferase substrate (65 mg/kg; VivoGloTM Luciferin, Promega, USA), the anesthetized mice were imaged using an *in vivo* imaging system (NightOWL L983; Berthold Technologies GmbH & Co KG, Germany). Luciferase signals were visualized and quantified using IndiGO^{TM} ver. 2.0.0.22 (Berthold Technologies GmbH & Co KG) imaging software for NightOWL.

2.10. Mouse xenograft study for tumor growth and lymph node metastasis

To evaluate tumor growth inhibition *in vivo*, SJCRH30-luc cells (3×10^6 in HBSS) were implanted subcutaneously into the right flank of nude mice (CAnN.Cg-Foxn1<nu>/CrlCrlj nu/nu, Charles River Japan). Tumor volume (TV) was calculated using the formula: $TV = ab^2 / 2$, where a and b represent tumor length and width, respectively. Once the tumors had reached a volume of approximately 100 mm^3, animals were randomly assigned to two groups (n = 5) and treatment was initiated. Twice-weekly intravenous administration of CF172 (25 mg/kg per injection) was performed for 14 days.

For the detection of lymph node metastasis, the resected lymph nodes were sonicated and lysed with 100 μL of Cell Lysis Buffer (Cell Signaling, USA) containing a complete protease inhibitor cocktail (Roche Diagnostics, Germany). The same amount of Bright-Glo luciferase assay system (Promega) was added. Assays were quantified by reading luminescence using EnVision spectrophotometer (PerkinElmer).

2.11. Statistical analyses

Statistical tests in this study were performed using Student's *t*-test or the Mann-Whitney U test. $P < 0.05$ was considered significant. Statistical analyses were performed using the SAS preclinical package (version 8.2; SAS Institute Inc., USA).

3. Results

3.1. CF172 specifically binds to and neutralizes human CXCR4

First, the author generated a monoclonal antibody against human CXCR4, which was designated CF172, as described in the Materials and Methods.

The binding activity of CF172 to human CXCR4 was determined by FACS using human CXCR4-expressing CHO cells (Fig. 2-1a). To evaluate the binding specificity of CF172 against human CXCR4, the author conducted FACS analysis using CHO cells expressing mouse CXCR4 and human CXCR2 (The protein most closely related to CXCR4). Results indicated that CF172 did not bind to either mouse CXCR4- or human CXCR2-expressing CHO cells (Fig. 2-1b and 2-1c, respectively).

Next, the author investigated the neutralizing activity of CF172 against human CXCR4 by using cell-based assays, as described in Materials and Methods. CF172 dose-dependently inhibited SDF1-mediated signaling of human CXCR4 (Fig. 2-2a). Additionally, CF172 did not inhibit CXCL8-mediated signaling of human CXCR2 (Fig. 2-2b), which was consistent with the observed binding specificity presented in Fig. 2-1.

3.2. SJCRH30 and RH30 are CXCR4-expressing rhabdomyosarcoma cell lines

Next, to investigate CXCR4 expression on the cell surface of rhabdomyosarcoma cells, the author conducted FACS analysis of CF172 using 5 different rhabdomyosarcoma cell lines. SJCRH30 and RH30 cells expressed human CXCR4 and the expression levels of SJCRH30 cells were higher than those of RH30 (Fig. 2-3a). To confirm this expression pattern, the author performed western blot analysis (Fig. 2-3b). Consistent with the cell surface expression pattern (Fig. 2-3a), SJCRH30 cells exhibited the highest CXCR4 protein expression among the 5

rhabdomyosarcoma cell lines.

3.3. CF172 inhibits the biological activity of human CXCR4 in SJCRH30 cells

To evaluate the inhibitory activity of CF172 against the biological activity of CXCR4 in rhabdomyosarcoma cells, the author further analyzed SJCRH30 cells, which exhibited the highest CXCR4 expression (Fig. 2-3a and 2-3b), by determining their response to SDF1.

CXCR4 is known to transduce signals via the Giα-subunit of the heterotrimeric G protein complex, after stimulation by SDF1 (Rollins 1997). The prototypic function of Giα proteins is the binding to and inhibition of adenylyl cyclase-mediated cAMP production (Neves et al. 2002, Dwinell et al. 2004). To determine if this was also the case in human rhabdomyosarcoma cells, the author assessed whether activation of CXCR4 with SDF1 could block adenylyl cyclase-mediated cAMP production in SJCRH30 cells. SJCRH30 cells were first incubated with SDF1 and then stimulated with forskolin, to upregulate cAMP production. As observed in Fig. 2-4a (comparison of (+) and (-) dotted line), SDF1 inhibited the forskolin-stimulated cAMP responses in SJCRH30 cells. The subsequent addition of CF172 abrogated the inhibition of forskolin-stimulated cAMP production by SDF1 in a dose-dependent manner (Fig. 2-4a).

CXCR4/SDF1 signaling in tumor cells is known to enhance migration activity (Muller et al. 2001, Burger and Kipps 2006, Oda et al. 2007, Akashi et al. 2008, Joyce and Pollard 2009). To determine if this was also the case in human rhabdomyosarcoma cells, the author assessed whether CXCR4 activation by SDF1 enhanced SJCRH30 cell migration activity. My results indicated that SDF1 enhanced

the migration activity of SJCRH30 cells (Fig. 2-4b). Addition of CF172 inhibited the SDF1-induced migration activity of SJCRH30 cells (Fig. 2-4b). To determine whether CF172 specifically inhibited migration and did not affect the proliferation of SJCRH30 cells, the author next investigated the effect of this agent on the proliferation of SJCRH30 cells. As shown in Fig. 2-5, serial concentrations of CF172 did not inhibit the proliferation of SJCRH30 cells in the presence or absence of SDF1.

3.4. CF172 inhibited *in vivo* peritoneal metastasis and lymph node metastasis of SJCRH30 cells

The author finally investigated the *in vivo* effect of CF172 against metastasis using SJCRH30 cells. Although there are many types of tumor metastasis, the author selected peritoneal metastasis and lymph node metastasis for evaluation because both peritoneal metastasis and lymph node metastasis are clinically observed with rhabdomyosarcoma. For these analyses, the author generated a SJCRH30 cell line stably expressing luciferase (SJCRH30-luc) in order to conduct bioimaging in mice (Fig. 2-6a). Compared to the SJCRH30 parental cells, the SJCRH30-luc cells exhibited similar levels of CXCR4 expression *in vitro* (Fig. 2-3 and Fig. 2-6b). In addition, the author evaluated SDF1-induced migration activity of SJCRH30-luc cells and found that SJCRH30-luc cell migration was induced by SDF1, while CF172 inhibited it (Fig. 2-6c).

The author then attempted to generate an experimental peritoneal metastasis model of rhabdomyosarcoma by intraperitoneally injecting SJCRH30-luc cells into nude mice. On the 5^{th} day after the inoculation of SJCRH30-luc cells, the author detected photons in the peritonea of inoculated nude mice. The amount of photons was not reduced by washing of the peritonea with PBS (data not shown). Therefore, the

author concluded that these results validated the experimental peritoneal metastasis model of rhabdomyosarcoma.

The author then performed an *in vivo* efficacy study involving intravenous administration of 25 mg/kg CF172, using the model described above. Briefly, SJCRH30-luc cells were intraperitoneally injected into nude mice. On the same day, CF172 (25 mg/kg) was intravenously injected as a single shot. On the 5^{th} day, peritoneal metastasis was evaluated by detection of photons, using bioimaging. My results indicated a significant reduction in the amount of photons in the CF172-injected mice when compared with the vehicle-injected mice ($p < 0.05$, Fig. 2-7a). The individual photos of mice on day 5 are presented in Fig. 2-5b ($n = 7$ in the vehicle-injected group and $n = 9$ in the CF172-injected group). In addition, the author evaluated the concentration of SDF1 in ascites fluid before and after the inoculation of SJCRH30-luc cells. As shown in Fig. 8, the SDF1 concentration before the inoculation of SJCRH30-luc cells did not differ from that after the inoculation of SJCRH30-luc cells. These data indicate that inoculation of SJCRH30-luc cells had little impact on the SDF1 concentration in ascites fluid. Thus, the effect of CF172 against peritoneal metastasis of SJCRH30-luc cells did not involve a dramatic change in SDF1 induced by inoculation of SJCRH30-luc cells.

The author then examined whether CF172 inhibited lymph node metastasis of SJCRH30-luc cells. SJCRH30-luc cells were implanted subcutaneously into the right flank of nude mice. Once the tumors reached a volume of approximately 100 mm^3, the mice were randomized into two groups ($n = 5$), and were administered CF172 (25 mg/kg) twice-weekly intravenously for 14 days. There was little difference in the size of the tumors formed by SJCRH30-luc cells in the primary lesion between the

CF172-injected and the vehicle-injected mice (Fig. 2-9a). In contrast, as shown in Fig. 2-9b, CF172 significantly inhibited lymph node metastasis of SJCRH30-luc cells in this model. These data further indicate that CF172 decreased the metastasis of SJCRH30-luc cells by inhibiting tumor migration from the primary lesion without affecting tumor volume.

4. Discussion

Tumor metastasis is an important clinical determinant in the prognosis of many tumors, while the overall cure rate of metastatic rhabdomyosarcoma remains very low, compared to localized rhabdomyosarcoma (Koscielniak et al. 1992, Crist et al. 2001, Breneman et al. 2003, Stevens et al. 2005, Oberlin et al. 2008, Malempati and Hawkins 2012). Therefore, therapeutic modalities capable of inhibiting tumor metastasis would be highly beneficial in the treatment of rhabdomyosarcoma. High CXCR4 expression correlates with metastatic incidence and poor prognosis of rhabdomyosarcoma (Diomedi-Camassei et al. 2008), suggesting that the SDF1/CXCR4 axis is very important for the metastatic process. These findings also suggest that an anti-CXCR4 antibody would be a promising agent for metastatic rhabdomyosarcoma treatment.

In this study, the author generated a novel anti-CXCR4 monoclonal antibody, CF172, which specifically binds and neutralizes human CXCR4. Several studies indicated that SDF1 activates downstream signaling pathways by interacting with the second extracellular loop of CXCR4 (Doranz et al. 1999, Brelot et al. 2000, Zhou et al. 2001, Huang et al. 2003, Kofuku et al. 2009). When comparing the amino acid sequences of human and mouse CXCR4, the second extracellular loop of CXCR4 exhibits lower sequence identity (67%) than other extracellular regions (Nagasawa et al. 1996). Additionally, CF172 did not bind to mouse CXCR4 (Fig. 2-1b). Collectively, these results suggested that CF172 binds to the second extracellular loop of CXCR4, thereby exhibiting specific binding reactivity and inhibiting SDF1-mediated signal transduction.

By using CF172, the author demonstrated that SJCRH30 and RH30 cells were the

CXCR4-expressing rhabdomyosarcoma cells among the 5 different cell lines evaluated (Fig. 2-3). Both of these cell lines are histologically characterized as alveolar-type rhabdomyosarcoma, while the remaining 3 cell lines are characterized as the embryonal-type (Charrasse et al. 2004). The alveolar-type is known to be a more aggressive rhabdomyosarcoma than the embryonal-type (Newton et al. 1995, Leuschner and Harms 1999, Oberlin et al. 2008). The findings in this study that CXCR4 is preferentially expressed in the alveolar-type are consistent with previously published data indicating that high CXCR4 expression correlates with poor prognosis in rhabdomyosarcoma (Diomedi-Camassei et al. 2008). These findings also suggested the importance of CXCR4 in rhabdomyosarcoma.

One of the most important findings was that CF172 inhibits the metastasis in two experimental rhabdomyosarcoma models (Fig. 2-7 and Fig. 2-9). Previous studies demonstrated that the SDF1 concentration in the peritoneum and lymph node is high (Muller et al. 2001, Yasumoto et al. 2006), suggesting that this high concentration of SDF1 enhances peritoneal and lymph node metastasis in rhabdomyosarcoma. The findings in this study that blocking the CXCR4/SDF1 axis by CF172 inhibited these metastases are consistent with this hypothesis and strongly support previously published conclusions that the CXCR4/SDF1 axis is important for tumor metastasis (Muller et al. 2001, Burger and Kipps 2006, Oda et al. 2007, Akashi et al. 2008, Joyce and Pollard 2009). These findings further suggest that the importance of CXCR4/SDF1 axis in tumor metastasis is also applicable to rhabdomyosarcoma.

Compared to localized rhabdomyosarcoma, high mortality rates are still observed in patients with metastatic rhabdomyosarcoma, despite aggressive multimodality therapy (Koscielniak et al. 1992, Crist et al. 2001, Breneman et al. 2003, Stevens et

al. 2005, Oberlin et al. 2008, Malempati and Hawkins 2012). Therefore, new therapeutic agents for metastatic rhabdomyosarcoma are still necessary, and my finding that CF172 has potential as a therapeutic antibody for metastatic rhabdomyosarcoma is of significance.

In conclusion, the results of the present study implicate CXCR4 signaling in the promotion of metastasis in rhabdomyosarcoma and CF172 was identified as a potential therapeutic antibody against metastatic rhabdomyosarcoma.

5. Figures

(a)

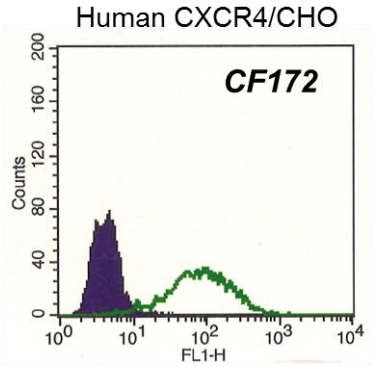

(b) **(c)**

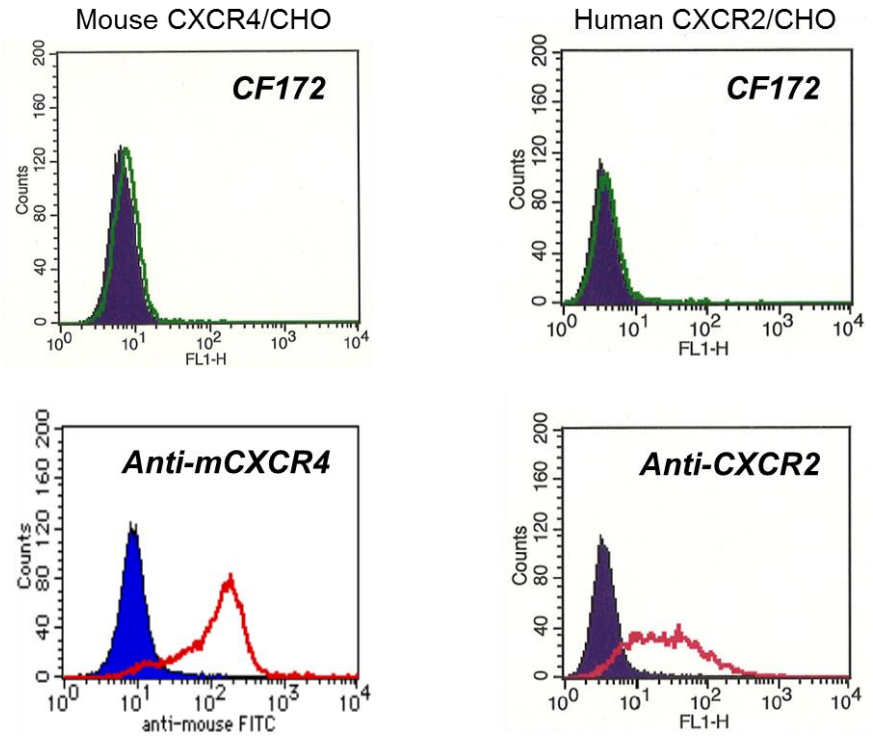

Fig. 2-1. Reaction specificity of CF172 against human CXCR4.

The binding activity of CF172 to CHO cells stably expressing (a) human CXCR4, (b) mouse CXCR4 and (c) human CXCR2, was measured by flow cytometry. Background binding, measured with isotype control (solid area), is also shown.

(a) CXCR4-bla U2OS

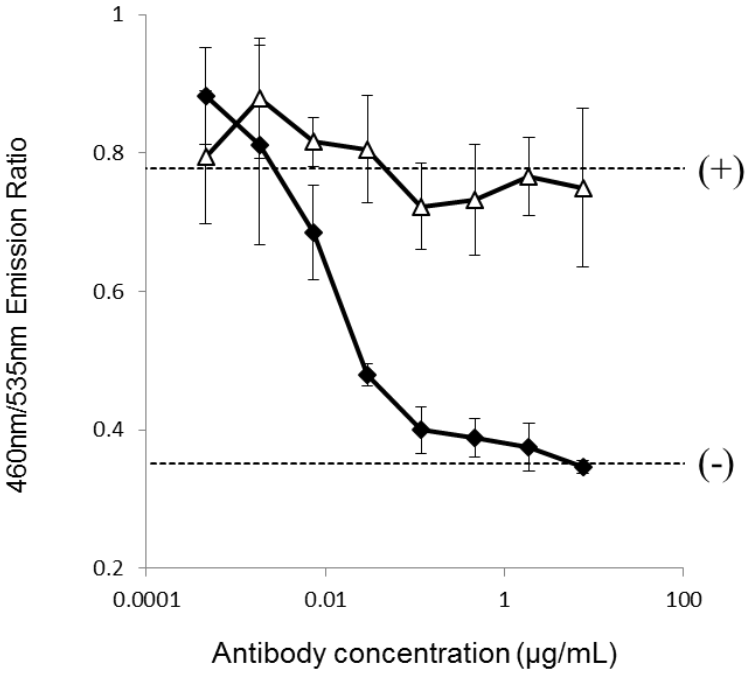

(b) CHO-K1 CXCR2

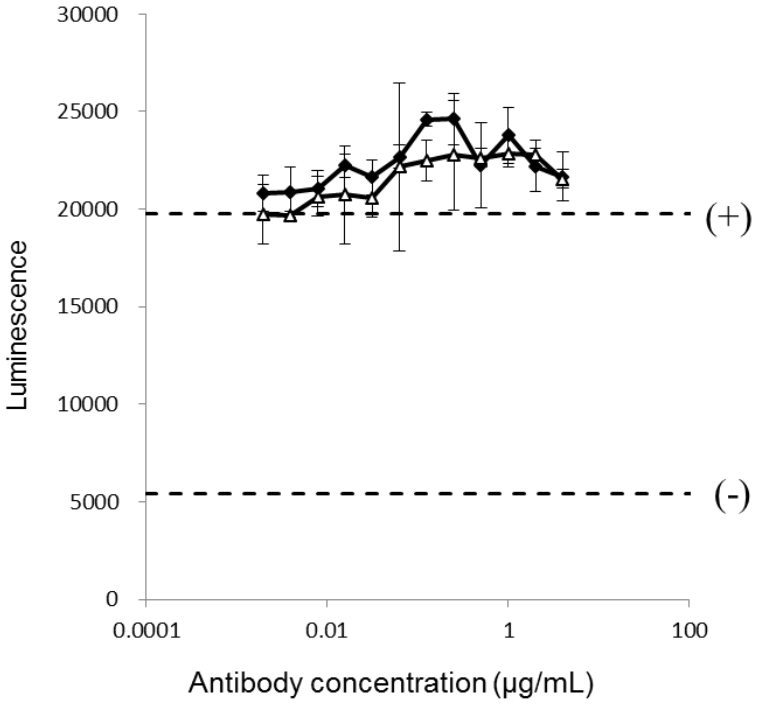

Fig. 2-2. Neutralization activity of CF172 against human CXCR4.

The neutralization activity of CF172 for CXCR4 was measured using a cell-based assay. (a) Tango CXCR4-bla U2OS cells were incubated overnight at 37°C, followed by 5 h incubation in the presence of SDF1 (4 nM) and serially diluted CF172 (◆) or mIgG2b control (△). Samples were then incubated for 2 h with LiveBLAzer FRET B/G substrate. Signals for 4 or 0 nM of SDF1 with no antibody are indicated by the (+) or (-) dotted lines, respectively. (b) PathHunter CHO-K1 CXCR2 cells were incubated overnight at 37°C followed by 90 min incubation in the presence of CXCL8 (1.25 nM) and serially diluted CF172 (◆) or mIgG2b control (△). Samples were then incubated 1 h with PathHunter detection reagent. The signals for 1.25 or 0 nM of CXCL8 with no antibody are indicated by the (+) or (-) dotted lines, respectively. All points indicate the mean ± SD (n = 3).

(a)

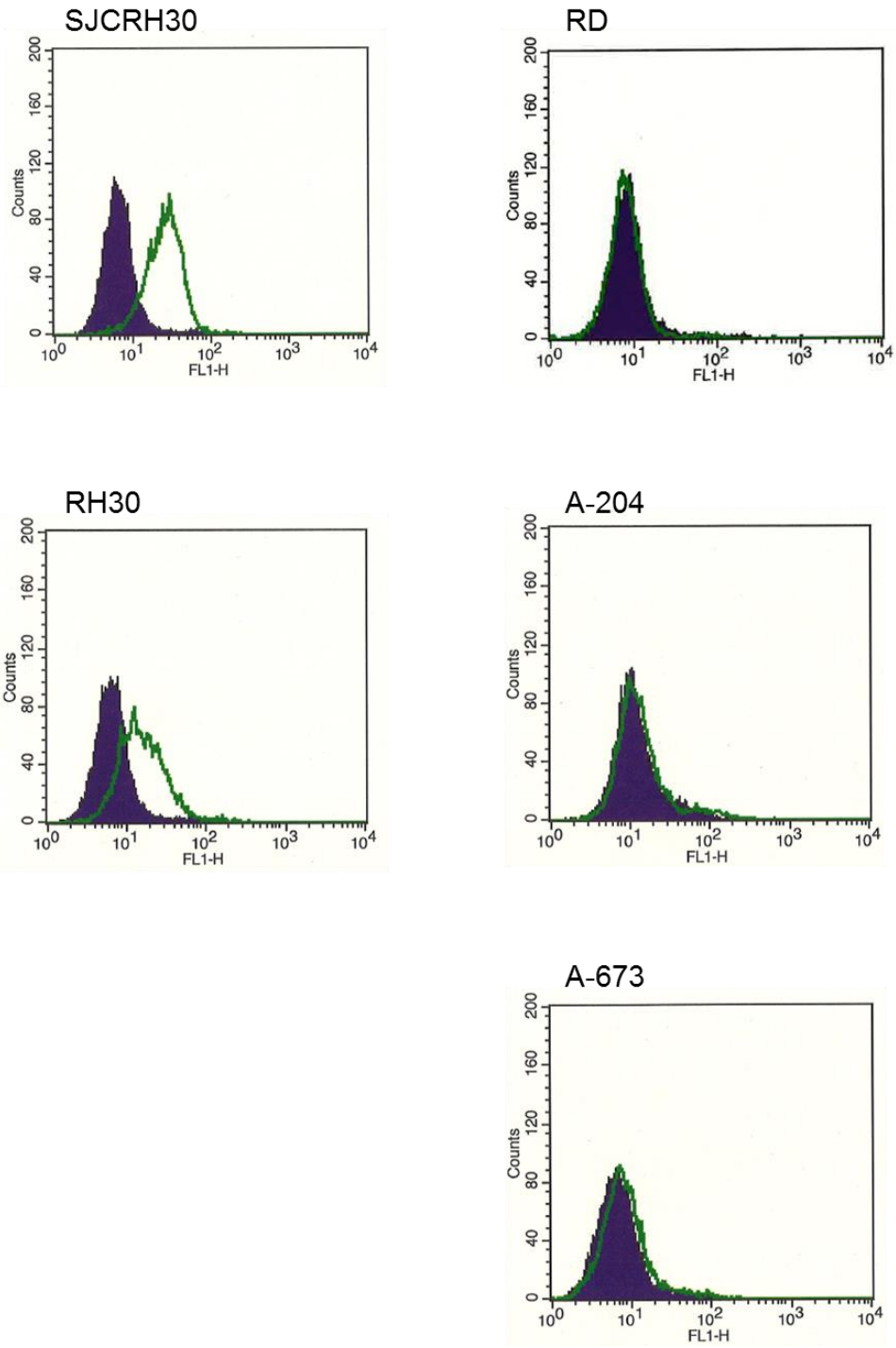

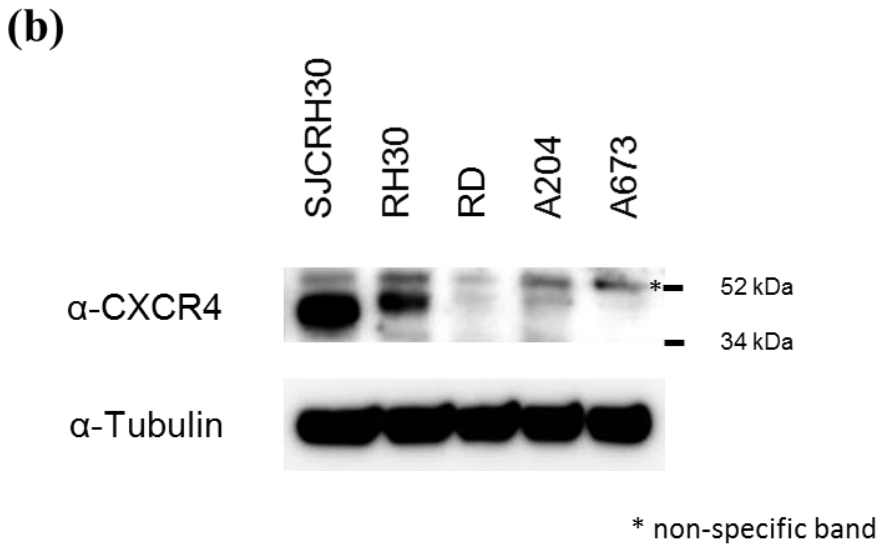

Fig. 2-3. Analysis of CXCR4 expression in rhabdomyosarcoma cell lines.

(a) CXCR4 membrane expression in rhabdomyosarcoma cell lines was analyzed by flow cytometry using CF172. Background binding, measured with isotype control (solid area), is also shown. (b) Expression of CXCR4 protein in 5 rhabdomyosarcoma cell lines was analyzed by western blot using anti-CXCR4 antibody.

(a)

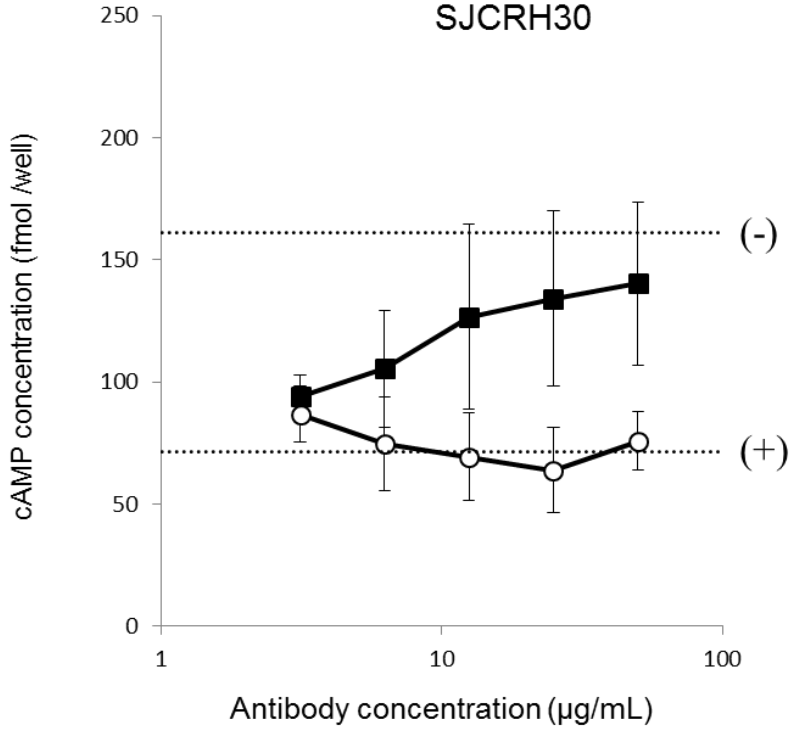
SJCRH30
cAMP concentration (fmol /well)
250
200
150
100
50
0
(-)
(+)
1
10
100
Antibody concentration (μg/mL)

(b)

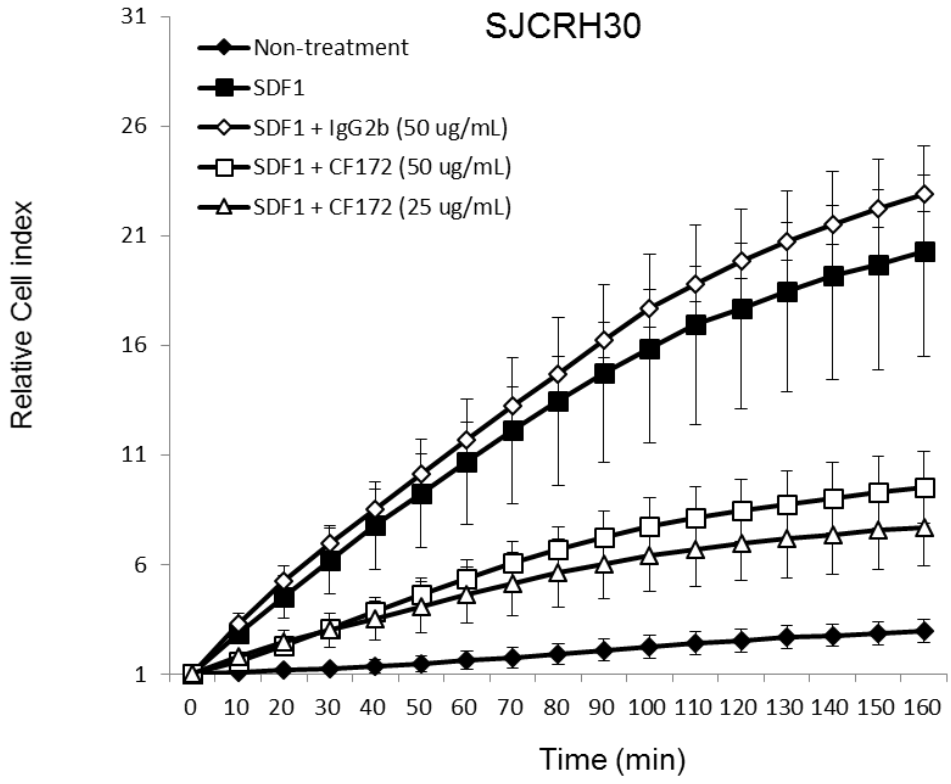
SJCRH30
Non-treatment
SDF1
SDF1 + IgG2b (50 ug/mL)
SDF1 + CF172 (50 ug/mL)
SDF1 + CF172 (25 ug/mL)
Relative Cell index
31
26
21
16
11
6
1
0 10 20 30 40 50 60 70 80 90 100 110 120 130 140 150 160
Time (min)

Fig.2-4. Inhibitory activity of CF172 against biological activity of CXCR4 in SJCRH30.

The ability of CF172 to inhibit biological activity of CXCR4 was measured using (a) SDF1/CXCR4-induced inhibitory activity of forskolin-stimulated cAMP production, and (b) SDF1/CXCR4-induced migration activity. (a) SJCRH30 cells were pretreated with serially diluted CF172 (■) or mIgG2b control (◯). Following this, cells were stimulated with 100 nM SDF1 and 25 μM forskolin. Cells were harvested 10 min later, and cAMP levels were assayed by ELISA. The signals for forskolin (25 μM) with 100 or 0 nM of SDF1, with no antibody, are indicated by the (+) or (-) dotted lines, respectively. (b) The xCELLigence system was used to monitor real-time cell migration. SJCRH30 cells with antibodies were seeded in the upper chamber of a CIM-Plate in the growth medium. The upper chamber was then placed on the lower chamber of the CIM-Plate containing 10 nM SDF1. Cell migration was monitored up to 7 h. All points indicate the mean ± SD (n = 3).

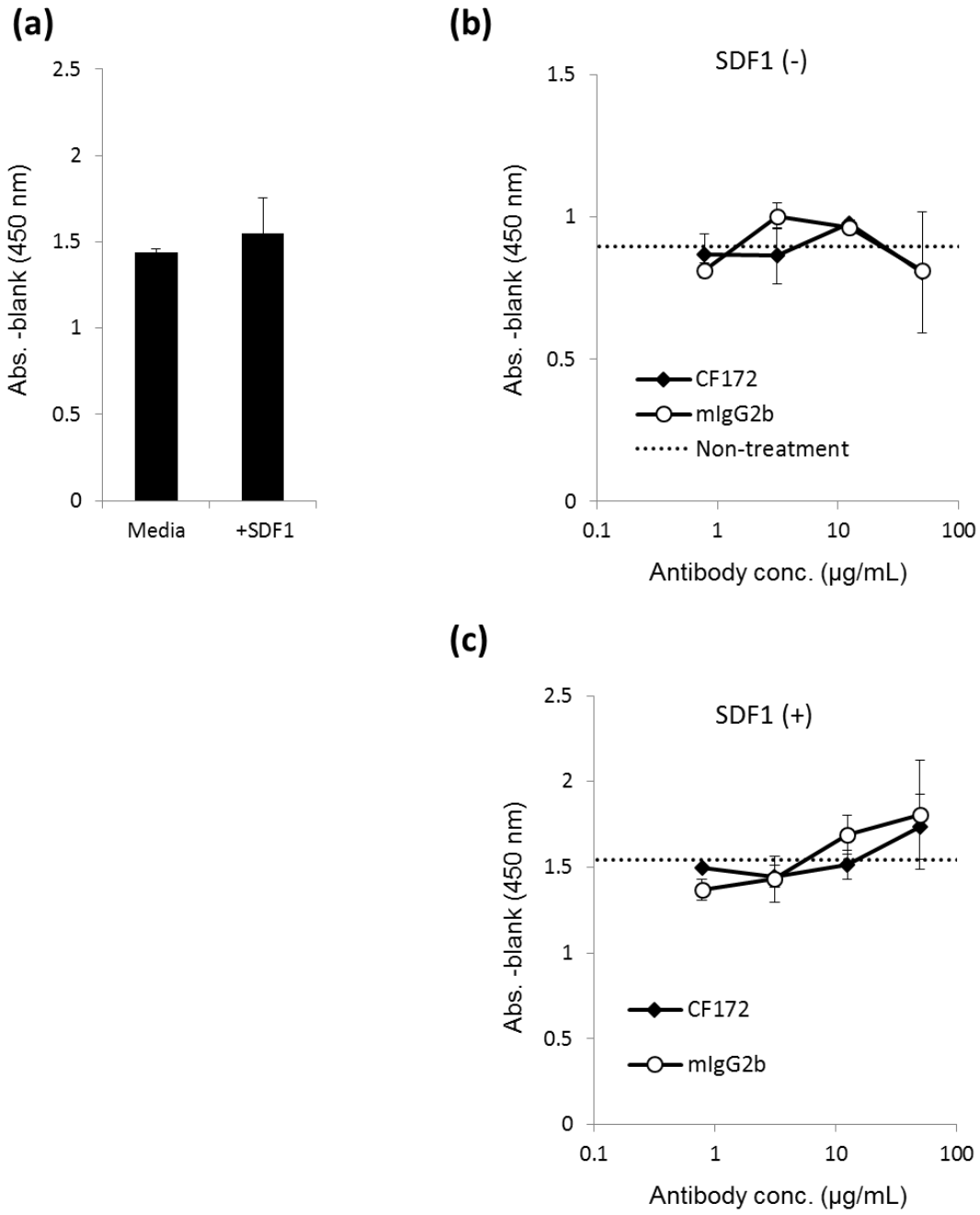

Fig. 2-5. Growth inhibition activity of CF172 against SJCRH30 cells.

(a) SJCRH30 cells were incubated with or without 100 nM of SDF1 for 96 h. The number of living cells was then determined using Cell Counting Kit-8 solution. SJCRH30 cells were incubated with serially diluted CF172 (◆) and mIgG2b control (◯) and (b) without 100 nM SDF1 or (c) with 100 nM SDF1 for 96 h. The number of living cells was then determined using Cell Counting Kit-8 solution. The cell number when 0 ng/mL antibody was added is indicated by the dotted line.

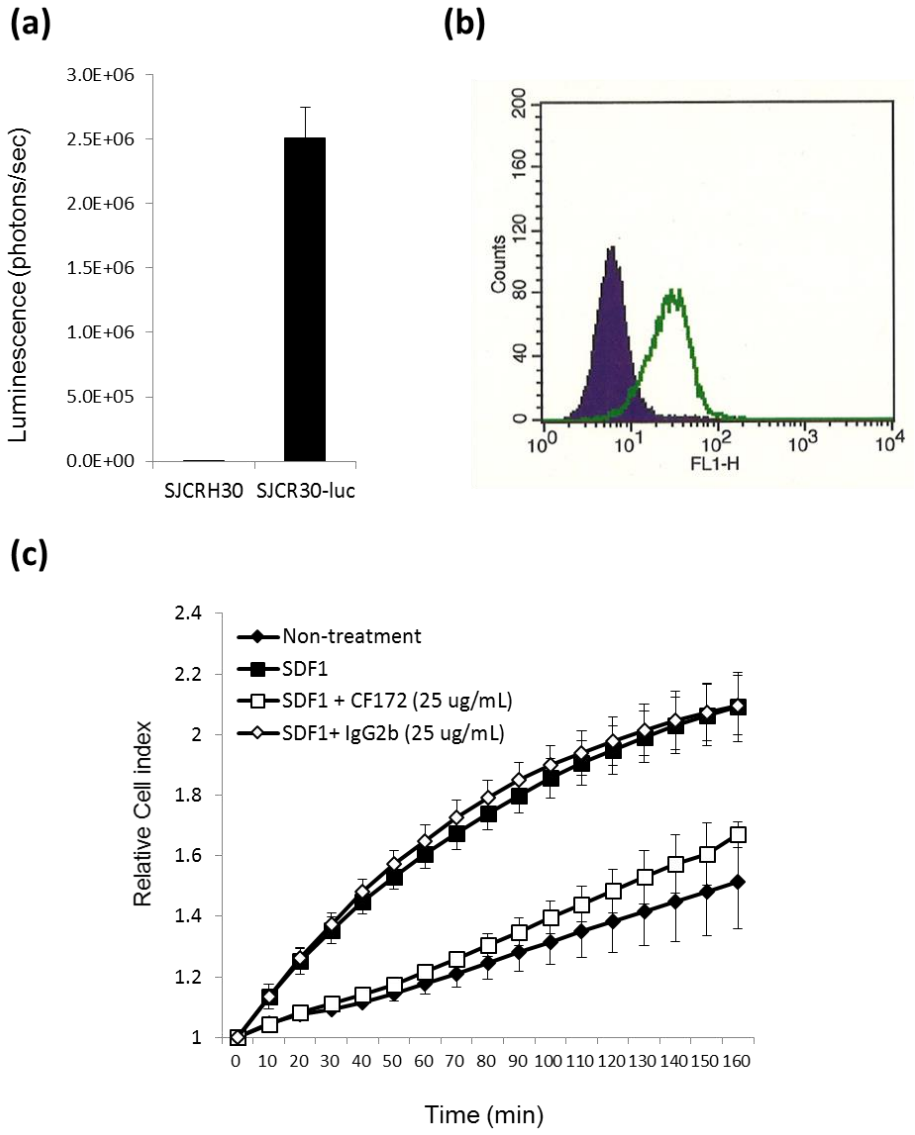

Fig. 2-6. Comparison of profile of SJCRH30 and SJCRH30-luc cells.

(a) SJCRH30-luc was generated by transfection with a luciferase expression vector. Luciferase activity was confirmed by the Bright-Glo luciferase assay system (n = 3 for each cell line). (b) CXCR4 membrane expression in SJCRH30-luc was analyzed by flow cytometry using CF172. The background binding determined using the isotype control (solid area) is also shown. (c) The xCELLigence system was used to monitor real-time cell migration. SJCRH30-luc cells with antibodies were seeded in the growth medium in the upper chamber of a CIM-Plate. The upper chamber was then placed on the lower chamber of the CIM-Plate containing 10 nM SDF-1α. Cell migration was monitored over a period of up to 7 h. All points indicate the mean ± SD (n = 3).

(a)

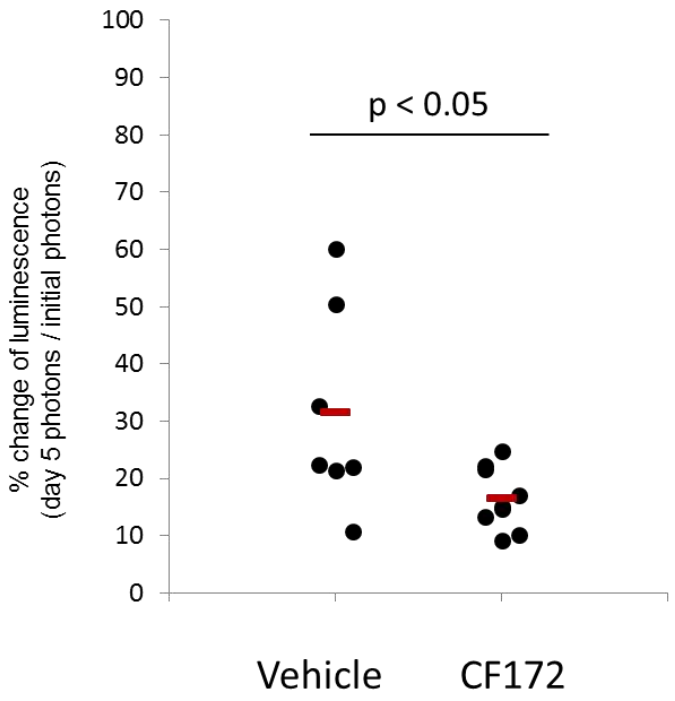
100
90
80
70
60
50
40
30
20
10
0
% change of luminescence
(day 5 photons / initial photons)
p < 0.05
Vehicle
CF172

(b)

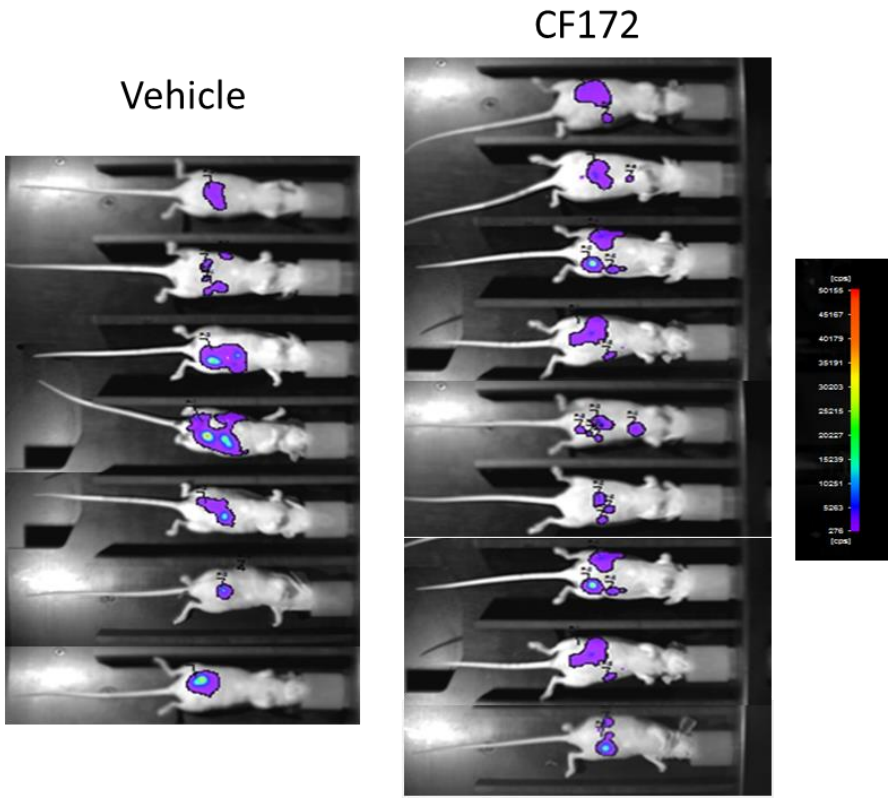
Vehicle
CF172

Fig. 2-7. *In vivo* effect of CF172 against peritoneal metastasis of CXCR4-expressing rhabdomyosarcoma model.

(a) The anti-peritoneal metastasis activity of CF172 against SJCRH30-luc cells was evaluated based on photon detection via bioimaging. SJCRH30-luc cells were intraperitoneally inoculated into nude mice. On the same day, CF172 (25 mg/kg) was intravenously injected in a single shot. After 5 days, metastasized tumor cells were measured by administration of luciferase substrate and detection of the photons. Data were individually plotted by % change from initial photon concentrations. Statistical tests were performed using Student's t-test. (b) Photographs of all mice on day 5.

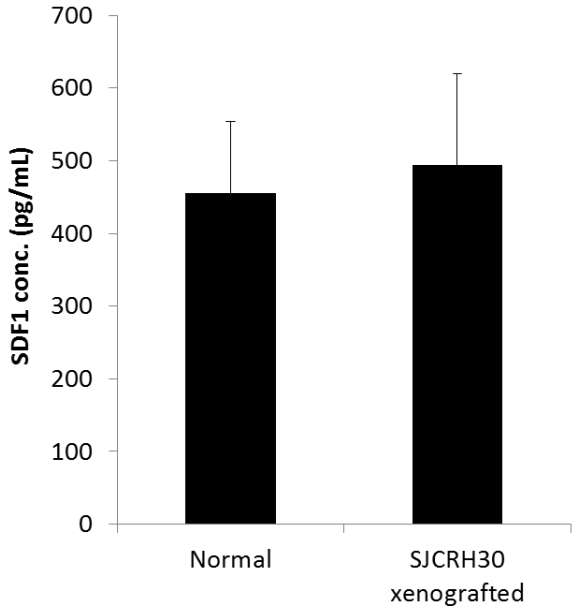

Fig. 2-8. Comparison of SDF1 concentration in ascites fluid of normal mice and SJCRH30-luc-xenografted mice.

SDF1 concentration in ascites fluid of normal mice and SJCRH30-luc-xenografted mice was analyzed by Quantikine CXCL12/SDF-1 alpha ELISA kit (R&D systems). Assay was performed by n = 5. All values are expressed as the mean ± SD.

(a)

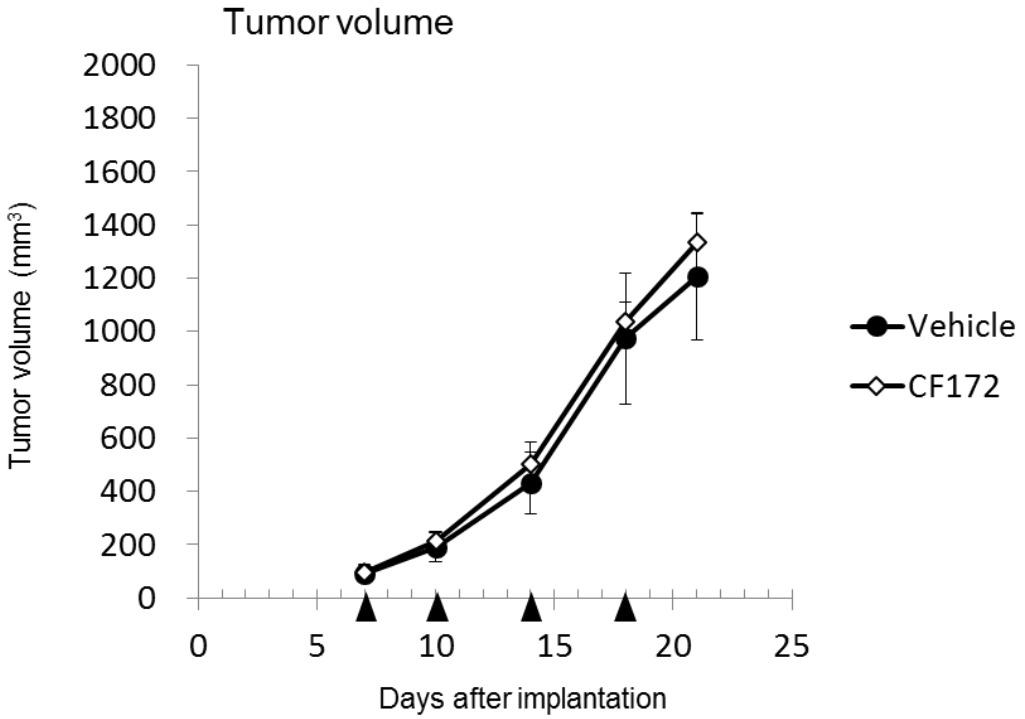
Tumor volume
Tumor volume (mm3)
2000
1800
1600
1400
1200
1000
800
600
400
200
0
0
5
10
15
20
25
Days after implantation
Vehicle
CF172

(b)

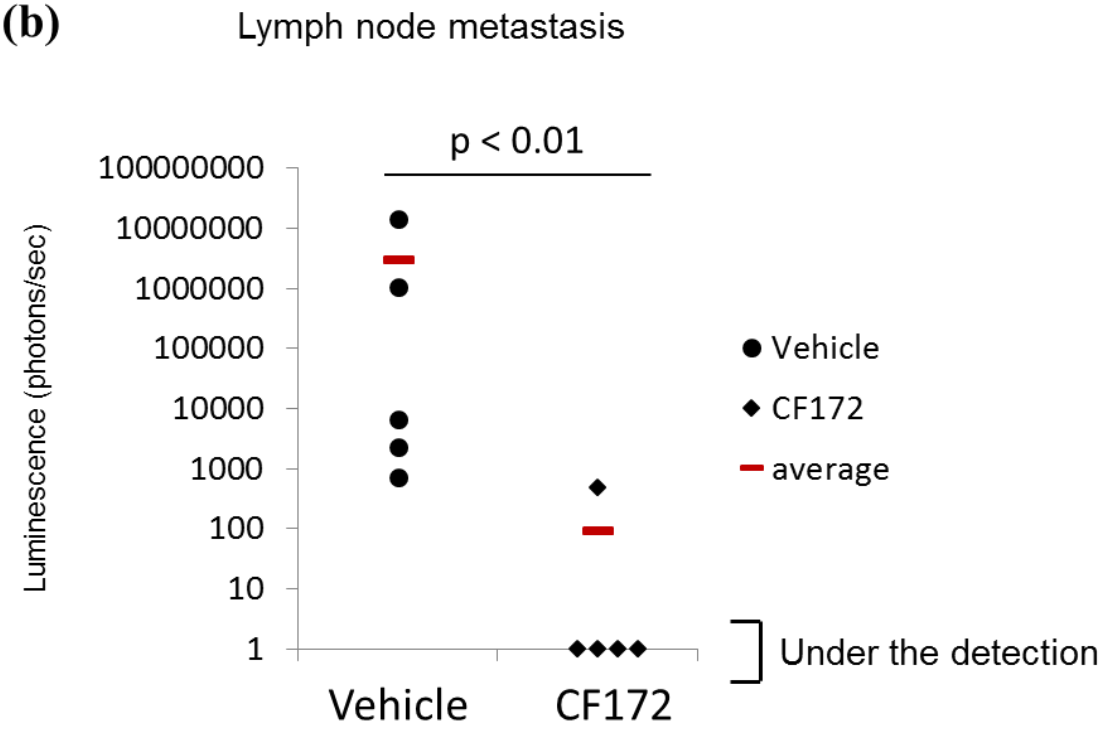
Lymph node metastasis
p < 0.01
Luminescence (photons/sec)
100000000
10000000
1000000
100000
10000
1000
100
10
1
Vehicle
CF172
Vehicle
CF172
average
Under the detection

Fig. 2-9. *In vivo* effect of CF172 against tumor growth and lymph node metastasis of CXCR4-expressing rhabdomyosarcoma model.

(a) Antitumor activity activity of CF172 against SJCRH30-luc cells was evaluated using subcutaneously implanted SJCRH30-luc cells. Once the tumors had reached a volume of approximately 100 mm^3, mice were randomly assigned to two groups (n = 5) and twice-weekly intravenous administration of CF172 (25 mg/kg) was performed for 14 days. The mean tumor volume is shown. Black triangle indicates administration day. (b) The anti-metastasis activity of CF172 against lymph node metastasis of SJCRH30-luc was evaluated by detection of photons from lysed lymph nodes. Statistical tests were performed using the Wilcoxon test.

General Conclusion

Tumor metastasis is an important determinant for tumor death and therapeutic modalities capable of inhibiting tumor metastasis should be beneficial for the treatment of many tumors. However, to date, no anti-metastatic drug is available.

In this study, the author identified two anti-metastatic monoclonal antibodies, cVE199 and CF172, which specifically target VEGF-D and CXCR4, respectively. Both antibodies presented anti-metastatic activities in animal models.

In Chapter I, the author developed cVE199, a monoclonal antibody with specific reactivity to human VEGF-D (Fig. 1-1). The cVE199 molecule decreased the lymphatic metastasis through inhibition of tumor lymph vessel formation (Fig. 1-8). With regard to targeting tumor vessels, VEGF-A targeted therapies (e.g. anti-VEGF-A antibody: bevacizumab) that inhibit tumor blood vessel formation, showed a potent antitumor activity in preclinical models (Presta et al. 1997, Borgstrom et al. 1998, McMahon 2000, Mendel et al. 2000, Wood et al. 2000). Indeed anti-VEGF-A antibody, bevacizumab, has been clinically used for many tumor types (Hurwitz et al. 2004, Giantonio et al. 2007, Saltz et al. 2008, Leighl et al. 2010, Chang et al. 2011, Batchelor et al. 2014, Pujade-Lauraine et al. 2014, von Minckwitz et al. 2014). However recent preclinical studies suggested that inhibition of VEGF-A signaling is accompanied by increased invasiveness and metastasis (Casanovas et al. 2005, Ebos et al. 2009, Paez-Ribes et al. 2009). The precise mechanisms of the exaggerated aggressiveness by VEGF-A targeted therapies are unknown, but a contributing factor could be hypoxia. Some reports showed that hypoxia promoted epithelial-mesenchymal transition (EMT) and EMT is believed to be a mechanism by which cancer cells become migratory and invasive (Sahlgren et al. 2008, Yang et al. 2008, Zhang et al. 2013). Other group reported that hypoxia upregulated the

transcription of c-Met, the tyrosine kinase receptor for hepatocyte growth factor (HGF) (Pennacchietti et al. 2003, Hara et al. 2006, Sennino et al. 2012). The c-Met/HGF signal transduction pathway plays a crucial role in controlling invasive growth of tumor cells. Thus, blood vessel inhibition is accompanied by increasing the number of malignant metastatic cells through hypoxia. Although cVE199 did not showed antitumor activity to primary tumors (Fig. 1-8a), the antibody significantly decreased lymphatic metastasis in an animal model through reduction of lymphangiogenesis. Therefore, targeting lymph vessels may be a better approach to generate anti-metastasis drugs.

In Chapter II, the author developed CF172, a monoclonal antibody with specific reactivity to human CXCR4 (Fig. 2-1, 2-2). CF172 decreased metastasis by inhibiting tumor migration from the primary lesion without affecting tumor volume (Fig. 2-7, 2-9). Although there is no clinically used drug that target chemotaxis of tumors, matrix metalloproteinases (MMP) inhibitors present a similar mechanism of action. MMP degrade collagen and proteoglycans, the components of the extracellular matrix (ECM). ECM physically inhibits tumor chemotaxis. Thus, MMP-overexpressing-tumors present an increased chemotaxis activity through ECM degradation (Curran and Murray 1999, Johansson et al. 2000, Kerkela and Saarialho-Kere 2003). Many MMP inhibitors (e.g., Marimastat and BAY12-9566) have been tested in human clinical studies. However, no compound has been approved as an antitumor drug. Although many reasons for the lack of success of MMP inhibitors in clinical trials were considered, a contributing factor could be toxicity. The most frequent side-effect associated with MMP inhibitors in clinical trials was a musculoskeletal syndrome (MSS) that manifested as pain and immobility in the shoulder joints, arthralgias, contractures in the hands, and an overall reduced quality of life for patients. A current theory is that the side-effects are predominantly related to off-

target metal chelation (Maquoi et al. 2004, Corbitt et al. 2007, Fingleton 2008, Li and Wu 2010). Many efforts have been made to generate MMP inhibitors that have improved selectivity. However, there is no successful example in clinical trials. Therefore, MMPs seem to be tough targets to generate drug candidates. On the other hand, CF172 specifically reacts to human CXCR4 and inhibits tumor metastasis in rhabdomyosarcoma models. Therefore, CXCR4 inhibition by CF172 may be a better approach to generate anti-metastasis drugs to target tumor chemotaxis.

Both cVE199 and CF172 did not inhibit tumor growth. Thus, the combination of antitumor drugs (e.g., cytotoxic agents) with each antibody may be a better approach for cancer treatment. Alternatively, although cVE199 and CF172 showed anti-metastatic activities, both antibodies did not completely inhibit metastasis (Fig. 1-8, 2-7, 2-9). Both antibodies inhibited different steps of tumor metastasis. Thus, the combination of both antibodies seems better than monotherapy to completely inhibit metastasis, if the tumor expresses both VEGF-D and CXCR4.

There is no molecular target agent for neuroblastoma and rhabdomyosarcoma treatment, which are the possible target indications of cVE199 and CF172 (Morgenstern et al. 2013, Hettmer et al. 2014). Therefore, my antibodies are of significance not only as novel anti-metastasis agents, but also as novel molecular target agents for these tumor types. Furthermore, the identified cVE199 and CF172 antibodies are highly specific to VEGF-D and CXCR4, respectively. Thus, these antibodies are useful not only for the development of drugs, but also as tools to understand the biological roles of each target protein, e.g., VEGF-D and CXCR4.

Acknowledgments

The author thanks Taeko Masuda, Asuka Motoda and Sachiya Yamamoto for their technical support; Mina Takahashi, Tsukasa Suzuki, Atsushi Narita, Tetsuya Wakabayashi and Takeshi Baba for antibody generation; and Junichi Nezu, Keiko Esaki, Akihisa Sakamoto, Manabu Wada, Masakazu Hasegawa, Naohiro Yabuta, Kunihiro Hattori, Masahiro Aoki, Hiroshi Sakamoto and Osamu Kondoh for helpful discussions.

Finally, the author expresses his deepest gratitude to Associate Professor Hidekazu Kuwayama, Tsukuba University, for his peer-review and invaluable advice.

References

Achen, M. G., et al. (1998). "Vascular endothelial growth factor D (VEGF-D) is a ligand for the tyrosine kinases VEGF receptor 2 (Flk1) and VEGF receptor 3 (Flt4)." Proc Natl Acad Sci U S A **95**(2): 548-553.

Achen, M. G. and S. A. Stacker (2008). "Molecular control of lymphatic metastasis." Ann N Y Acad Sci **1131**: 225-234.

Akashi, T., et al. (2008). "Chemokine receptor CXCR4 expression and prognosis in patients with metastatic prostate cancer." Cancer Sci **99**(3): 539-542.

Allemani, C., et al. (2015). "Global surveillance of cancer survival 1995-2009: analysis of individual data for 25,676,887 patients from 279 population-based registries in 67 countries (CONCORD-2)." Lancet **385**(9972): 977-1010.

Balkwill, F. (2004). "Cancer and the chemokine network." Nat Rev Cancer **4**(7): 540-550.

Batchelor, T. T., et al. (2014). "Antiangiogenic therapy for glioblastoma: current status and future prospects." Clin Cancer Res **20**(22): 5612-5619.

Bergers, G. and L. E. Benjamin (2003). "Tumorigenesis and the angiogenic switch." Nat Rev Cancer **3**(6): 401-410.

Bockhorn, M., et al. (2007). "Active versus passive mechanisms in metastasis: do cancer cells crawl into vessels, or are they pushed?" Lancet Oncol **8**(5): 444-448.

Borgstrom, P., et al. (1998). "Neutralizing anti-vascular endothelial growth factor antibody completely inhibits angiogenesis and growth of human prostate carcinoma micro tumors in vivo." Prostate **35**(1): 1-10.

Brelot, A., et al. (2000). "Identification of residues of CXCR4 critical for human immunodeficiency virus coreceptor and chemokine receptor activities." J Biol Chem **275**(31): 23736-23744.

Breneman, J. C., et al. (2003). "Prognostic factors and clinical outcomes in children and adolescents with metastatic rhabdomyosarcoma--a report from the Intergroup Rhabdomyosarcoma Study IV." J Clin Oncol **21**(1): 78-84.

Brodeur, G. M. (2003). "Neuroblastoma: biological insights into a clinical enigma." Nat Rev Cancer **3**(3): 203-216.

Burger, J. A. and T. J. Kipps (2006). "CXCR4: a key receptor in the crosstalk between tumor cells and their microenvironment." Blood **107**(5): 1761-1767.

Casanovas, O., et al. (2005). "Drug resistance by evasion of antiangiogenic targeting of VEGF signaling in late-stage pancreatic islet tumors." Cancer Cell **8**(4): 299-309.

Chang, G. C., et al. (2011). "Comparative effectiveness of bevacizumab plus cisplatin-based chemotherapy versus pemetrexed plus cisplatin treatment in East Asian non-

squamous non-small cell lung cancer patients applying real-life outcomes." Asia Pac J Clin Oncol **7 Suppl 2**: 34-40.

Charrasse, S., et al. (2004). "Variation in cadherins and catenins expression is linked to both proliferation and transformation of Rhabdomyosarcoma." Oncogene **23**(13): 2420-2430.

Chung, M. K., et al. (2010). "Correlation between lymphatic vessel density and regional metastasis in squamous cell carcinoma of the tongue." Head Neck **32**(4): 445-451.

Corbitt, C. A., et al. (2007). "Mechanisms to inhibit matrix metalloproteinase activity: where are we in the development of clinically relevant inhibitors?" Recent Pat Anticancer Drug Discov **2**(2): 135-142.

Crist, W. M., et al. (2001). "Intergroup rhabdomyosarcoma study-IV: results for patients with nonmetastatic disease." J Clin Oncol **19**(12): 3091-3102.

Curran, S. and G. I. Murray (1999). "Matrix metalloproteinases in tumour invasion and metastasis." J Pathol **189**(3): 300-308.

de Manzoni, G., et al. (1996). "Prognostic significance of lymph node dissection in gastric cancer." Br J Surg **83**(11): 1604-1607.

Detmar, M. and S. Hirakawa (2002). "The formation of lymphatic vessels and its importance in the setting of malignancy." J Exp Med **196**(6): 713-718.

Diomedi-Camassei, F., et al. (2008). "Clinical significance of CXC chemokine receptor-4 and c-Met in childhood rhabdomyosarcoma." Clin Cancer Res **14**(13): 4119-4127.

Doranz, B. J., et al. (1999). "Identification of CXCR4 domains that support coreceptor and chemokine receptor functions." J Virol **73**(4): 2752-2761.

Dudjak, L. A. (1992). "Cancer metastasis." Semin Oncol Nurs **8**(1): 40-50.

Dwinell, M. B., et al. (2004). "SDF-1/CXCL12 regulates cAMP production and ion transport in intestinal epithelial cells via CXCR4." Am J Physiol Gastrointest Liver Physiol **286**(5): G844-850.

Ebos, J. M., et al. (2009). "Accelerated metastasis after short-term treatment with a potent inhibitor of tumor angiogenesis." Cancer Cell **15**(3): 232-239.

Fidler, I. J. (1999). "Critical determinants of cancer metastasis: rationale for therapy." Cancer Chemother Pharmacol **43 Suppl**: S3-10.

Fidler, I. J. (2002). "Critical determinants of metastasis." Semin Cancer Biol **12**(2): 89-96.

Fidler, I. J. and L. M. Ellis (2000). "Chemotherapeutic drugs--more really is not better." Nat Med **6**(5): 500-502.

Fingleton, B. (2008). "MMPs as therapeutic targets--still a viable option?" Semin Cell

Dev Biol **19**(1): 61-68.

Frech, S., et al. (2009). "Lymphatic vessel density in correlation to lymph node metastasis in head and neck squamous cell carcinoma." Anticancer Res **29**(5): 1675-1679.

Ghaferi, A. A., et al. (2009). "Prognostic significance of a positive nonsentinel lymph node in cutaneous melanoma." Ann Surg Oncol **16**(11): 2978-2984.

Giantonio, B. J., et al. (2007). "Bevacizumab in combination with oxaliplatin, fluorouracil, and leucovorin (FOLFOX4) for previously treated metastatic colorectal cancer: results from the Eastern Cooperative Oncology Group Study E3200." J Clin Oncol **25**(12): 1539-1544.

Grandi, C., et al. (1985). "Prognostic significance of lymphatic spread in head and neck carcinomas: therapeutic implications." Head Neck Surg **8**(2): 67-73.

Hara, S., et al. (2006). "Hypoxia enhances c-Met/HGF receptor expression and signaling by activating HIF-1alpha in human salivary gland cancer cells." Oral Oncol **42**(6): 593-598.

Hettmer, S., et al. (2014). "Rhabdomyosarcoma: current challenges and their implications for developing therapies." Cold Spring Harb Perspect Med **4**(11): a025650.

Huang, X., et al. (2003). "Molecular dynamics simulations on SDF-1alpha: binding with CXCR4 receptor." Biophys J **84**(1): 171-184.

Hurwitz, H., et al. (2004). "Bevacizumab plus irinotecan, fluorouracil, and leucovorin for metastatic colorectal cancer." N Engl J Med **350**(23): 2335-2342.

Johansson, N., et al. (2000). "Matrix metalloproteinases in tumor invasion." Cell Mol Life Sci **57**(1): 5-15.

Joyce, J. A. and J. W. Pollard (2009). "Microenvironmental regulation of metastasis." Nat Rev Cancer **9**(4): 239-252.

Juttner, S., et al. (2006). "Vascular endothelial growth factor-D and its receptor VEGFR-3: two novel independent prognostic markers in gastric adenocarcinoma." J Clin Oncol **24**(2): 228-240.

Kashima, K., et al. (2012). "Inhibition of lymphatic metastasis in neuroblastoma by a novel neutralizing antibody to vascular endothelial growth factor-D." Cancer Sci **103**(12): 2144-2152.

Ke, N., et al. (2011). "The xCELLigence system for real-time and label-free monitoring of cell viability." Methods Mol Biol **740**: 33-43.

Kerkela, E. and U. Saarialho-Kere (2003). "Matrix metalloproteinases in tumor progression: focus on basal and squamous cell skin cancer." Exp Dermatol **12**(2): 109-125.

Kirkin, V., et al. (2001). "Characterization of indolinones which preferentially inhibit

VEGF-C- and VEGF-D-induced activation of VEGFR-3 rather than VEGFR-2." Eur J Biochem **268**(21): 5530-5540.

Kofuku, Y., et al. (2009). "Structural basis of the interaction between chemokine stromal cell-derived factor-1/CXCL12 and its G-protein-coupled receptor CXCR4." J Biol Chem **284**(50): 35240-35250.

Koscielniak, E., et al. (1992). "Metastatic rhabdomyosarcoma and histologically similar tumors in childhood: a retrospective European multi-center analysis." Med Pediatr Oncol **20**(3): 209-214.

Kucia, M., et al. (2004). "CXCR4-SDF-1 signalling, locomotion, chemotaxis and adhesion." J Mol Histol **35**(3): 233-245.

Leighl, N. B., et al. (2010). "Efficacy and safety of bevacizumab-based therapy in elderly patients with advanced or recurrent nonsquamous non-small cell lung cancer in the phase III BO17704 study (AVAiL)." J Thorac Oncol **5**(12): 1970-1976.

Leppanen, V. M., et al. (2011). "Structural determinants of vascular endothelial growth factor-D receptor binding and specificity." Blood **117**(5): 1507-1515.

Leuschner, I. and D. Harms (1999). "[Pathology of childhood and adolescent rhabdomyosarcoma]." Pathologe **20**(2): 87-97.

Li, X. and J. F. Wu (2010). "Recent developments in patent anti-cancer agents targeting the matrix metalloproteinases (MMPs)." Recent Pat Anticancer Drug Discov **5**(2): 109-141.

Liotta, L. A. (1992). "Cancer cell invasion and metastasis." Sci Am **266**(2): 54-59, 62-53.

Liu, B., et al. (2008). "Lymphangiogenesis and its relationship with lymphatic metastasis and prognosis in malignant melanoma." Anat Rec (Hoboken) **291**(10): 1227-1235.

Lughezzani, G., et al. (2009). "Prognostic significance of lymph node invasion in patients with metastatic renal cell carcinoma: a population-based perspective." Cancer **115**(24): 5680-5687.

Malempati, S. and D. S. Hawkins (2012). "Rhabdomyosarcoma: review of the Children's Oncology Group (COG) Soft-Tissue Sarcoma Committee experience and rationale for current COG studies." Pediatr Blood Cancer **59**(1): 5-10.

Maquoi, E., et al. (2004). "Anti-invasive, antitumoral, and antiangiogenic efficacy of a pyrimidine-2,4,6-trione derivative, an orally active and selective matrix metalloproteinases inhibitor." Clin Cancer Res **10**(12 Pt 1): 4038-4047.

Maris, J. M. (2010). "Recent advances in neuroblastoma." N Engl J Med **362**(23): 2202-2211.

Maris, J. M., et al. (2007). "Neuroblastoma." Lancet **369**(9579): 2106-2120.

McMahon, G. (2000). "VEGF receptor signaling in tumor angiogenesis." Oncologist **5**

Suppl 1: 3-10.

Mendel, D. B., et al. (2000). "The angiogenesis inhibitor SU5416 has long-lasting effects on vascular endothelial growth factor receptor phosphorylation and function." Clin Cancer Res **6**(12): 4848-4858.

Modak, S. and N. K. Cheung (2010). "Neuroblastoma: Therapeutic strategies for a clinical enigma." Cancer Treat Rev **36**(4): 307-317.

Morgenstern, D. A., et al. (2013). "Current and future strategies for relapsed neuroblastoma: challenges on the road to precision therapy." J Pediatr Hematol Oncol **35**(5): 337-347.

Muller, A., et al. (2001). "Involvement of chemokine receptors in breast cancer metastasis." Nature **410**(6824): 50-56.

Nagasawa, T., et al. (1996). "Molecular cloning and characterization of a murine pre-B-cell growth-stimulating factor/stromal cell-derived factor 1 receptor, a murine homolog of the human immunodeficiency virus 1 entry coreceptor fusin." Proc Natl Acad Sci U S A **93**(25): 14726-14729.

Nakamura, Y., et al. (2003). "Prognostic significance of vascular endothelial growth factor D in breast carcinoma with long-term follow-up." Clin Cancer Res **9**(2): 716-721.

Neves, S. R., et al. (2002). "G protein pathways." Science **296**(5573): 1636-1639.

Newton, W. A., Jr., et al. (1995). "Classification of rhabdomyosarcomas and related sarcomas. Pathologic aspects and proposal for a new classification--an Intergroup Rhabdomyosarcoma Study." Cancer **76**(6): 1073-1085.

Nguyen, T. H. (2004). "Mechanisms of metastasis." Clin Dermatol **22**(3): 209-216.

Oberlin, O., et al. (2008). "Prognostic factors in metastatic rhabdomyosarcomas: results of a pooled analysis from United States and European cooperative groups." J Clin Oncol **26**(14): 2384-2389.

Oda, Y., et al. (2007). "Prognostic implications of the nuclear localization of Y-box-binding protein-1 and CXCR4 expression in ovarian cancer: their correlation with activated Akt, LRP/MVP and P-glycoprotein expression." Cancer Sci **98**(7): 1020-1026.

Ono, N., et al. (2012). "Preclinical antitumor activity of the novel heat shock protein 90 inhibitor CH5164840 against human epidermal growth factor receptor 2 (HER2)-overexpressing cancers." Cancer Sci **103**(2): 342-349.

Paez-Ribes, M., et al. (2009). "Antiangiogenic therapy elicits malignant progression of tumors to increased local invasion and distant metastasis." Cancer Cell **15**(3): 220-231.

Paget, S. (1989). "The distribution of secondary growths in cancer of the breast. 1889." Cancer Metastasis Rev **8**(2): 98-101.

Pantel, K. and R. H. Brakenhoff (2004). "Dissecting the metastatic cascade." Nat Rev Cancer **4**(6): 448-456.

Pennacchietti, S., et al. (2003). "Hypoxia promotes invasive growth by transcriptional activation of the met protooncogene." Cancer Cell **3**(4): 347-361.

Presta, L. G., et al. (1997). "Humanization of an anti-vascular endothelial growth factor monoclonal antibody for the therapy of solid tumors and other disorders." Cancer Res **57**(20): 4593-4599.

Pujade-Lauraine, E., et al. (2014). "Bevacizumab combined with chemotherapy for platinum-resistant recurrent ovarian cancer: The AURELIA open-label randomized phase III trial." J Clin Oncol **32**(13): 1302-1308.

Qin, L. X. and Z. Y. Tang (2002). "The prognostic significance of clinical and pathological features in hepatocellular carcinoma." World J Gastroenterol **8**(2): 193-199.

Raica, M. and D. Ribatti (2010). "Targeting tumor lymphangiogenesis: an update." Curr Med Chem **17**(8): 698-708.

Rollins, B. J. (1997). "Chemokines." Blood **90**(3): 909-928.

Rossi, D. and A. Zlotnik (2000). "The biology of chemokines and their receptors." Annu Rev Immunol **18**: 217-242.

Saharinen, P., et al. (2004). "Lymphatic vasculature: development, molecular regulation and role in tumor metastasis and inflammation." Trends Immunol **25**(7): 387-395.

Sahlgren, C., et al. (2008). "Notch signaling mediates hypoxia-induced tumor cell migration and invasion." Proc Natl Acad Sci U S A **105**(17): 6392-6397.

Saltz, L. B., et al. (2008). "Bevacizumab in combination with oxaliplatin-based chemotherapy as first-line therapy in metastatic colorectal cancer: a randomized phase III study." J Clin Oncol **26**(12): 2013-2019.

Sennino, B., et al. (2012). "Suppression of tumor invasion and metastasis by concurrent inhibition of c-Met and VEGF signaling in pancreatic neuroendocrine tumors." Cancer Discov **2**(3): 270-287.

Stacker, S. A., et al. (2001). "VEGF-D promotes the metastatic spread of tumor cells via the lymphatics." Nat Med **7**(2): 186-191.

Stacker, S. A., et al. (1999). "Biosynthesis of vascular endothelial growth factor-D involves proteolytic processing which generates non-covalent homodimers." J Biol Chem **274**(45): 32127-32136.

Stacker, S. A., et al. (2014). "Lymphangiogenesis and lymphatic vessel remodelling in

cancer." Nat Rev Cancer **14**(3): 159-172.

Stevens, M. C., et al. (2005). "Treatment of nonmetastatic rhabdomyosarcoma in childhood and adolescence: third study of the International Society of Paediatric Oncology--SIOP Malignant Mesenchymal Tumor 89." J Clin Oncol **23**(12): 2618-2628.

Strahm, B., et al. (2008). "The CXCR4-SDF1alpha axis is a critical mediator of rhabdomyosarcoma metastatic signaling induced by bone marrow stroma." Clin Exp Metastasis **25**(1): 1-10.

Thelen, A., et al. (2008). "VEGF-D promotes tumor growth and lymphatic spread in a mouse model of hepatocellular carcinoma." Int J Cancer **122**(11): 2471-2481.

Tuna, S., et al. (2011). "Prognostic significance of the metastatic lymph node ratio for survival in colon cancer." J BUON **16**(3): 478-485.

Veikkola, T., et al. (2001). "Signalling via vascular endothelial growth factor receptor-3 is sufficient for lymphangiogenesis in transgenic mice." EMBO J **20**(6): 1223-1231.

von Minckwitz, G., et al. (2014). "Bevacizumab plus chemotherapy versus chemotherapy alone as second-line treatment for patients with HER2-negative locally recurrent or metastatic breast cancer after first-line treatment with bevacizumab plus chemotherapy (TANIA): an open-label, randomised phase 3 trial." Lancet Oncol **15**(11): 1269-1278.

White, J. D., et al. (2002). "Vascular endothelial growth factor-D expression is an independent prognostic marker for survival in colorectal carcinoma." Cancer Res **62**(6): 1669-1675.

Wong, S. Y., et al. (2005). "Tumor-secreted vascular endothelial growth factor-C is necessary for prostate cancer lymphangiogenesis, but lymphangiogenesis is unnecessary for lymph node metastasis." Cancer Res **65**(21): 9789-9798.

Wood, J. M., et al. (2000). "PTK787/ZK 222584, a novel and potent inhibitor of vascular endothelial growth factor receptor tyrosine kinases, impairs vascular endothelial growth factor-induced responses and tumor growth after oral administration." Cancer Res **60**(8): 2178-2189.

Yang, M. H., et al. (2008). "Direct regulation of TWIST by HIF-1alpha promotes metastasis." Nat Cell Biol **10**(3): 295-305.

Yashiro, M., et al. (2009). "Effects of VEGFR-3 phosphorylation inhibitor on lymph node metastasis in an orthotopic diffuse-type gastric carcinoma model." Br J Cancer **101**(7): 1100-1106.

Yasumoto, K., et al. (2006). "Role of the CXCL12/CXCR4 axis in peritoneal

carcinomatosis of gastric cancer." Cancer Res **66**(4): 2181-2187.

Yeung, T. L., et al. (2015). "Cellular and molecular processes in ovarian cancer metastasis. A Review in the Theme: Cell and Molecular Processes in Cancer Metastasis." Am J Physiol Cell Physiol **309**(7): C444-456.

Yokoyama, Y., et al. (2003). "Expression of vascular endothelial growth factor (VEGF)-D and its receptor, VEGF receptor 3, as a prognostic factor in endometrial carcinoma." Clin Cancer Res **9**(4): 1361-1369.

Yokoyama, Y., et al. (2003). "Vascular endothelial growth factor-D is an independent prognostic factor in epithelial ovarian carcinoma." Br J Cancer **88**(2): 237-244.

Zhang, L., et al. (2013). "Hypoxia induces epithelial-mesenchymal transition via activation of SNAI1 by hypoxia-inducible factor -1alpha in hepatocellular carcinoma." BMC Cancer **13**: 108.

Zhou, N., et al. (2001). "Structural and functional characterization of human CXCR4 as a chemokine receptor and HIV-1 co-receptor by mutagenesis and molecular modeling studies." J Biol Chem **276**(46): 42826-42833.

List of publication

1. **Kashima K**, Watanabe M, Satoh Y, Hata J, Ishii N, Aoki Y.

Inhibition of lymphatic metastasis in neuroblastoma by a novel neutralizing antibody to vascular endothelial growth factor-D.

Cancer Sci. 2012; 103: 2144-52.

2. **Kashima K**, Watanabe M, Satoh Y, Hata J, Ishii N, Aoki Y.

Inhibition of metastasis of rhabdomyosarcoma by a novel neutralizing antibody to CXC chemokine receptor-4.

Cancer Sci. 2014; 105: 1343-50.